1959

Structures and phase equilibria of binary rare earth metal systems

Robert Michael Valletta
Iowa State University

STRUCTURES AND PHASE EQUILIBRIA OF BINARY RARE EARTH METAL SYSTEMS

by

Robert Michael Valletta

A Dissertation Submitted to the
Graduate Faculty in Partial Fulfillment of
The Requirements for the Degree of
DOCTOR OF PHILOSOPHY

Major Subject: Physical Chemistry

Approved:

Signature was redacted for privacy.

In Charge of Major Work

Signature was redacted for privacy.

Head of Major Department

Signature was redacted for privacy.

Dean of Graduate College

Iowa State University
of Science and Technology
Ames, Iowa

1959

TABLE OF CONTENTS

INTRODUCTION

Before the twentieth century, the rare earths occupied a unique, unexplainable position in the periodic table. The introduction of Bohr's quantum theory of the atom and further developments of quantum theory have shown the electron configuration of the rare earth metals to be in general $1s^2$, $2s^2$, $2p^6$, $3s^2$, $3p^6$, $3d^{10}$, $4s^2$, $4p^6$, $4d^{10}$, $4f^n$, $5s^2$, $5p^6$ and three conduction electrons. As chemical studies of these elements progressed, it became clear that this explanation was much too simple, since cerium and terbium showed higher valences under certain circumstances and samarium, europium and ytterbium could be di-valent. These discrepancies were explained by a tendency in these elements for the number of electrons in the 4f sub-shell to change. The increased stability of the atoms arising from the cancellation of orbital and magnetic moments when the 4f sub-shell is full or empty tends to stabilize states where a 4f electron has entered or left the sub-shell to approach the stable structure and it is these elements that show an anomalous valence. Orbital moments cancel when the sub-shell is 1/2 full, which explains the greater stability of the anomalous form of the elements on either side of gadolinium.

Early studies of the physical properties of the metals indicated that the factors determining structure were much more

complex than was originally believed. Magnetic studies of the ions and metals indicated that 4f electrons were shielded inside the atom and did not contribute appreciably to the valence electrons. The rare-earth metals commonly have three electrons taking part in the bonding through the conduction electrons. Since europium and ytterbium have an anomalous $4f^n$ configuration in the metal, they have two electrons in the conduction band and at low temperatures, it is possible to get 4 electrons in the conduction band for cerium. Because of the greater charge on the nucleus with increasing atomic number of the rare earth, all the electrons are pulled in closer to the nucleus and this results in a decreasing radius for these atoms with increasing atomic number. The bonding and directional properties of the valence electrons should be almost identical except for the shielding effect of the 4f electrons and the change in atomic size.

In recent years, the studies of Spedding and his coworkers on the separation of the rare-earth elements and the preparation of the pure metals in large quantities have made it possible to make much more exhaustive studies on the pure rare-earth metals and alloys. Although the availability of the rare earths has made it possible to study many of the properties of the pure rare earths, the behavior cannot be fitted quantitatively into the currently accepted theories of metals. Therefore, accumulation of extensive data on these interesting,

unique metals should be of great value in developing a better theory of metals.

The rare-earth metals are particularly suitable for such purposes since in alloy systems they form series of intermetallic compounds and solid solutions, which vary only slightly, as the rare-earth component is changed from alloy to alloy, and it is possible to hold certain variables more or less constant across the series. In such a series, it is possible to study the properties as a more continuous function of atomic size and atomic number than is possible with any other series of the periodic table.

The rare-earth metals may be divided into two groups on the basis of structure. Lanthanum, praseodymium and neodymium have hexagonal structures based on ABAC stacking of the planes of atoms. Cerium, although it is face centered cubic at room temperature, should be included in this group since it transforms to an ABAC structure at lower temperatures. The elements gadolinium through lutetium, with the exception of di-valent ytterbium, have the normal hexagonal ABAB structure. Samarium, which is not included in either group, has a close packed structure with a more complex stacking arrangement. It was commonly believed in the past that the rare-earth metals would form complete series of solid solutions in the intra-rare-earth alloys. However, complete solid solubility is only possible when the two rare earths crystallize with the same stacking arrangement. Even in this latter case, the deviation

from ideal solution might be larger than was originally thought. The existence of these various phases of the close packed system arising from different stacking should make these alloys particularly interesting since they would supply considerable information on the factors which determine the structures which exist.

Logically, the first system of this type to study is the lanthanum-gadolinium system since it includes the first elements of each group. The lanthanum-yttrium and gadolinium-yttrium systems should also be investigated for contrasting purposes. While yttrium is not a true rare earth, it closely resembles gadolinium in that it has 3 conduction electrons, crystallizes with the ABAB hexagonal close packed structure and has an atomic volume almost identical to gadolinium. Gadolinium has 4f electrons while lanthanum and yttrium do not. Lanthanum and gadolinium have incomplete 4f shells shielded by outer electrons while yttrium does not. Therefore, it should be possible with these systems to differentiate between factors determining bonding which depend on magnetic interactions and 4f electron contributions, as contrasted to those factors arising from atomic size and the conduction electrons.

A structure study of these alloys would also help to interpret the results of studies of other physical properties of the alloys, since magnetic, super-conductivity and linear expansion measurements have been performed recently on these three systems.

HISTORICAL

Pure Metals

The early literature on the rare earths is full of conflicting data as a result of the relatively impure metal studied by many investigators. It has only been in recent years that most of the ambiguities have been resolved as a result of the increased availability of pure rare-earth metals. Spedding et. al. (1950, 1951) and Spedding and Powell (1954) have described the ion-exchange method used to prepare the oxides of the rare earths with purities greater than 99.9 percent. Spedding and Daane (1954a, 1956) have also described the preparation of the pure metals in large quantities by the reduction of the anhydrous fluorides with calcium.

Lanthanum

The melting point of lanthanum was determined by Vogel and Neumann (1947) to be 915° C. They also reported a transformation at 830° C. Massenhausen (1952) reported the melting point of lanthanum as 863° C and a transition at 812° C. Vogel and Klose (1954) found that the melting point of a 97 percent lanthanum sample was 865° C and also found a solid transformation at 775° C. Spedding and Daane (1954a) report the melting point of greater than 99 percent lanthanum metal to be 920° C and a transformation at 868° C. A transformation at 868° C was also reported by Spedding et. al. (1957) as a

result of high temperature resistivity studies of lanthanum metal. They also found a resistivity anomaly at lower temperatures which they associated with a hexagonal close packed ABAC to face centered cubic transition. There was a great deal of hysteresis and the transition temperature range differed on heating and cooling. A transition with hysteresis had been found in resistivity studies by Trombe and Foex (1943). They report values of 150° C on cooling and 350° C on heating for this transition. Jaeger et. al. (1938) have also reported anomalies in resistivity data at 420° - 436° C, 560° C and 709° - 715° C and specific heat anomalies at 548° C, 655° C and 709° C. However, their results are questionable because of the large amount of iron present in their sample (97% La, 1% Fe).

McLennan and McKay (1930) reported lanthanum was hexagonal close packed with lattice parameters a = 3.72 A and c = 6.06 A. Quill (1932a) reported the structure of lanthanum as hexagonal close packed with lattice constants, a = 3.75 ± 0.01 A and c = 6.06 ± 0.03 A. Zintl and Neumayr (1933) reported that unannealed lanthanum gave a hexagonal close packed structure with very broad lines but after annealing for several days at 350° C, in vacuum, a face centered cubic pattern with a = 5.296 ± 0.002 A was obtained. They report the purity of the metal as 99.6 percent but their value for the melting point, 812° C, does not substantiate this claim. Rossi (1934) also reports the structure of lanthanum as originally

hexagonal close packed but after annealing at 350° C, it transformed to face centered cubic. He reports a = 3.75 A, c/a = 1.61 for the hexagonal form and a = 5.62-5.63 A for the face centered cubic phase which he claimed was due to a surface layer of lanthanum hydride. Klemm and Bommer (1937) reported a face centered cubic structure with the lattice constant, a = 5.294 A. This structure was again reported by Bommer (1939). Ziegler (1949) observed a diffuse hexagonal close packed phase and after annealing at 350° C, a sharp face centered cubic pattern. Young and Ziegler (1952) reported lanthanum annealed at 350° C as face centered cubic with a lattice constant, a = 5.291 ± 0.003 A. Ziegler et. al. (1953) again reported a diffuse hexagonal close packed pattern with unannealed metal and a face centered cubic pattern after annealing at 350°-400° C. The lattice constants were a = 3.74 ± 0.01 A and c = 6.06 ± 0.02 A for the hexagonal form and a = 5.285 ± 0.005 A for the cubic structure. James et. al. (1952) reported lanthanum to be a mixture of face centered cubic and hexagonal close packed with the hexagonal form predominating. Farr et. al. (1953) reported lanthanum as face centered cubic and attempts to obtain a hexagonal close packed structure were unsuccessful.

Recently Spedding et. al. (1956) have shown that lanthanum has a hexagonal structure, ABAC stacking, with lattice constants, a = 3.770 A and c = 12.159 A. Hanak (1959) in a study of the high temperature transitions of rare-earth metals reports lanthanum to be a mixture of the face centered

cubic and ABAC hexagonal phases at room temperature. He also reports a transition to face centered cubic on heating at 350° C and the reverse transition occurring at approximately 200° C. However, he was unable to obtain a pure hexagonal close packed structure at room temperature. He reports the high temperature form of lanthanum as body centered cubic and a transition temperature of approximately 862° C.

Gadolinium

The crystal structure of gadolinium has been reported by Klemm and Bommer (1937), Banister et. al. (1954) and Spedding et. al. (1956). They all report it to be hexagonal close packed. Spedding and Daane (1954) report the melting point to be 1327° C and a transition at approximately 1262° C. Hanak (1959) has also found evidence for a transition in gadolinium at 1262° C. Spedding and Daane (1954a) report the melting point to be approximately 1350° C. There is no evidence for crystal structure changes except that observed by Spedding and Daane and Hanak. The structure of the high temperature form is unknown.

Yttrium

Quill (1932a and 1932b) reported the structure of yttrium as hexagonal close packed with lattice constants a = 3.663 ± 0.008 A and c = 5.814 ± 0.012 A. Bommer (1939) also reported yttrium as hexagonal close packed with lattice constants a = 3.629 ± 0.004 A and c = 5.750 ± 0.007 A. Spedding et. al.

(1956) recently reported yttrium to be hexagonal close packed with lattice constants a = 3.6474 ± 0.0007 A and c = 5.7306 ± 0.0008 A. The melting point of yttrium, until recently, was open to question. The value has been determined to be between 1509° and 1550° C. Wakefield (1957) determined the melting point of yttrium containing approximately 2000 parts per million of oxygen and 1400 parts per million of tantalum as 1551° C by both the Pirani and Alterthum (1923) method and thermal analysis employing a platinum-platinum (13%) rhodium thermocouple. Recently, Habermann et. al. (1959) have determined the melting point of distilled yttrium as 1509° C. Evidence for a high temperature transformation in yttrium has been advanced by Eash (1959) and Gibson (1959). The transformation is reported to occur at 1490° C, very near the melting point.

Alloy Studies

Phase diagrams

The only intra-rare-earth alloy system which has been studied is the lanthanum-cerium system. Vogel and Klose (1954) report the lanthanum-cerium system shows complete solid solubility at room temperature.

They also show a region of complete solid solubility below the solidus indicating that the high temperature form of both metals is the same. Hanak (1959) has recently shown both

metals to be body centered cubic at temperatures near their melting points. Savitskii and Terekhova (1958) also state that lanthanum and cerium form solid solutions at room temperature. However, the phase diagram they propose shows no transition in the alloys to a high temperature structure.

Other alloy studies

In recent years the physical properties of binary alloy systems containing two rare-earth metals have been studied. Lock (1957) has studied the magnetic properties of lanthanum-neodymium alloys at low temperatures. Roberts and Lock (1957) have studied the specific heats and magnetic susceptibilities of lanthanum-cerium alloys at low temperatures. Thoburn et. al. (1958) measured the magnetic properties of lanthanum-gadolinium and gadolinium-yttrium alloys and Anderson et. al. (1958) have investigated the super-conductivity of lanthanum-yttrium and lanthanum-lutetium alloys. Thoburn et. al. (1958) report a phase in the lanthanum-gadolinium system whose structure they were unable to determine. Horn (1958) in a study of the thermal expansion of lanthanum-yttrium alloys, reported an interesting anomaly in an 85 atomic percent lanthanum-15 atomic percent yttrium alloy. A contraction in volume was observed in the temperature range from 50° to 110° C on heating. The transition did not appear after the sample was cooled to room temperature and immediately re-heated. However, it was found again in a heating cycle after the sample had been left

at room temperature in the apparatus for a week. Born is unable to explain this unusual behavior. Barton (1957), in a study of the vapor pressure of thulium and thulium-neodymium alloys reports a two phase region, h.c.p. Tm structure (ABAB stacking) plus h.c.p. Nd structure (ABAC stacking), at approximately 30 atomic percent thulium.

EXPERIMENTAL METHOD

Preparation of Alloys

The alloys studied in this investigation were made from the metals prepared by methods employed in the Ames Laboratory and described by Spedding and Daane (1954). This method can be briefly described as the reduction of anhydrous rare-earth fluorides by calcium in tantalum crucibles. Typical analysis of the metals and alloys is shown in Table 1. It should be noted in Table 1 that tantalum is much more soluble in the higher melting point metals, yttrium and gadolinium, than in the lower melting metals, lanthanum, cerium, praseodymium and neodymium. This trend continued in the alloys as can be seen in Table 1. It appears that alloying decreases the solubility of tantalum by a larger amount than that expected by the relatively lower melting point of the alloy compared to that of gadolinium or yttrium. Thus, although 0.2 percent tantalum was present in the yttrium, it is believed that tantalum was not present to more than 0.05 percent in any of the alloys.

Originally attempts were made to prepare the alloys by co-melting the metals in an arc furnace of the type described by Nash (1959), in which the recesses in a water-cooled copper hearth contained the sample and a piece of zirconium that was arc-melted to scavenge the helium atmosphere. The "buttons"

Table 1. Typical analysis of the pure metals and alloys

	Al	Be	Ca	Fe	Mg	Si	Ta
La	--[a]	--	.02[b]	--	.002	.01	--
Ce	--	--	.04	.006	.004	.01	--
Pr	--	--	.04	.006	--	.03	.03
Nd	.02	--	.02	.006	--	.03	.05
Gd	--	--	--	.01	--	.03	.1
Y	--	--	.04	.01	--	.05	.2
Alloy	--	--	--	.01	.01	.03	--

[a]Element not detected.

[b]All values are in percent.

formed after casting were inverted and re-melted several times in an attempt to insure homogeneity. However, X-ray diffraction patterns from the top and bottom of the samples showed that the alloys were not homogeneous. This was evident since the powder patterns did not have the same lattice constants and in some cases not even the same structure. This behavior precluded use of arc-melting for the preparation of the alloys.

The difficulty encountered in preparing homogeneous alloys was obviated by the following method. Pieces of metal weighing 5 grams or less were randomly placed in a tantalum crucible. The crucible was placed in a glass vacuum system which

was evacuated to at least 1 x 10^{-5} mm. of mercury. The crucible was gradually heated to the melting temperature of the highest melting component by radio-frequency induction heating, while a vacuum of at least 5 x 10^{-4} mm. of mercury was maintained during the outgassing of the crucible and its contents. This method of heating stirred the mixture rapidly in a radial direction. A tantalum stirring rod was lowered and raised rapidly through the molten mixture in order to prevent the formation of layers of varying composition throughout the length of molten mixture. The alloy was kept molten and stirred for approximately 15 minutes and then the sample was rapidly cooled to a temperature just below its melting point and annealed for approximately an hour. This method was used to prepare the majority of the alloys, but it was found later that homogeneous alloys could be prepared without vertical mixing by keeping the mixture molten for approximately an hour.

The homogeneity of the alloys was again checked by comparison of x-ray powder patterns of samples prepared from different parts of the alloy. The powder patterns obtained in this way were identical by visual comparison.

Thermal Analysis

Thermal analysis is one of the most valuable methods of studying high temperature transitions. However, two major limitations are inherent in this method: (1) The technique

can only be used for transitions with fairly large energy changes, (2) Thermal analysis does not tell the nature of the change. Since only the high temperature transitions of the alloys had large energies associated with them, it was possible to use this method only to study the alloys in the temperature range from 840° to 1550° C.

The lanthanum-yttrium and lanthanum-gadolinium samples weighed about 125 gms. and were contained in a tantalum crucible, 1" in diameter by 4½" long, made from 0.005 inches sheet, shown in Figure 1. The thermocouple well, A, 1/8" i.d. tantalum tubing, was cast into the sample, by weighting the tubing with a tantalum rod and allowing it to sink into the molten alloy, B. It was centered in the crucible by 3 tantalum spacers, C, 15/16" of an inch in diameter with a 3/16" diameter hole in the center. They were equally spaced in the crucible above the alloy, so that the tantalum thermocouple well remained in the center of the crucible when it sank into the molten alloy. The tantalum tubing was sealed at the bottom by welding in a 1/8" tantalum plug, D, which also served to raise the thermocouple junction 1/3 of the way from the bottom of the crucible to the top of the alloy and give good thermal contact between the thermocouple well and the thermocouple junction.

The crucibles employed in the thermal analysis of the gadolinium-yttrium system were 3/4" diameter tantalum crucibles

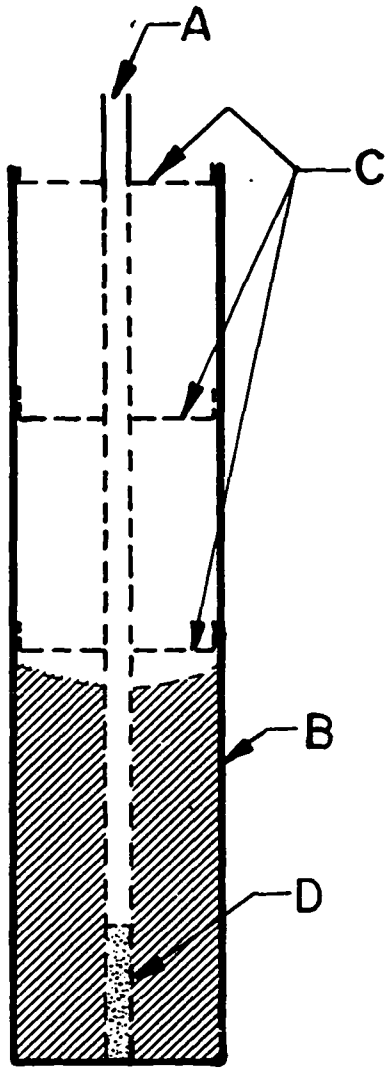

Figure 1. Crucible for thermal analysis

with 0.005" thick walls, containing 60 to 100 gms. of metal. The thermocouple well was made of 1/8" i.d. tantalum tubing sealed into the top cover of the crucible. The crucible was sealed with a helium atmosphere inside, so that the alloys could be heated to higher temperatures without gadolinium or yttrium distilling from the crucibles.

Pt-Pt (13%) Rh and chromel-alumel thermocouples, calibrated with copper, aluminum and lead samples obtained from the National Bureau of Standards, were used in the investigation. The thermocouples were rechecked after each thermal analysis against the standard copper sample. Generally the agreement was within $\pm$ 1° C; however, several times the calibration changed drastically ($\pm$ 10° C). When this happened, the thermocouple was discarded and the thermal analysis was re-run with a newly calibrated thermocouple.

The samples were heated in a vacuum or purified rare gas atmosphere in a tantalum tube resistor furnace that could be evacuated to 1×10^{-6} mm. of mercury. Figure 2 shows the essential details of the heating element and crucible stand. Figure 2 is not drawn to scale to emphasize the more important details of the part of the furnace shown in the drawing. The graphite block shown in Figure 2 was replaced by a molybdenum block for the gadolinium-yttrium alloys. The graphite block was originally used since a high melting point, low vapor pressure metal block was not available and graphite was chosen

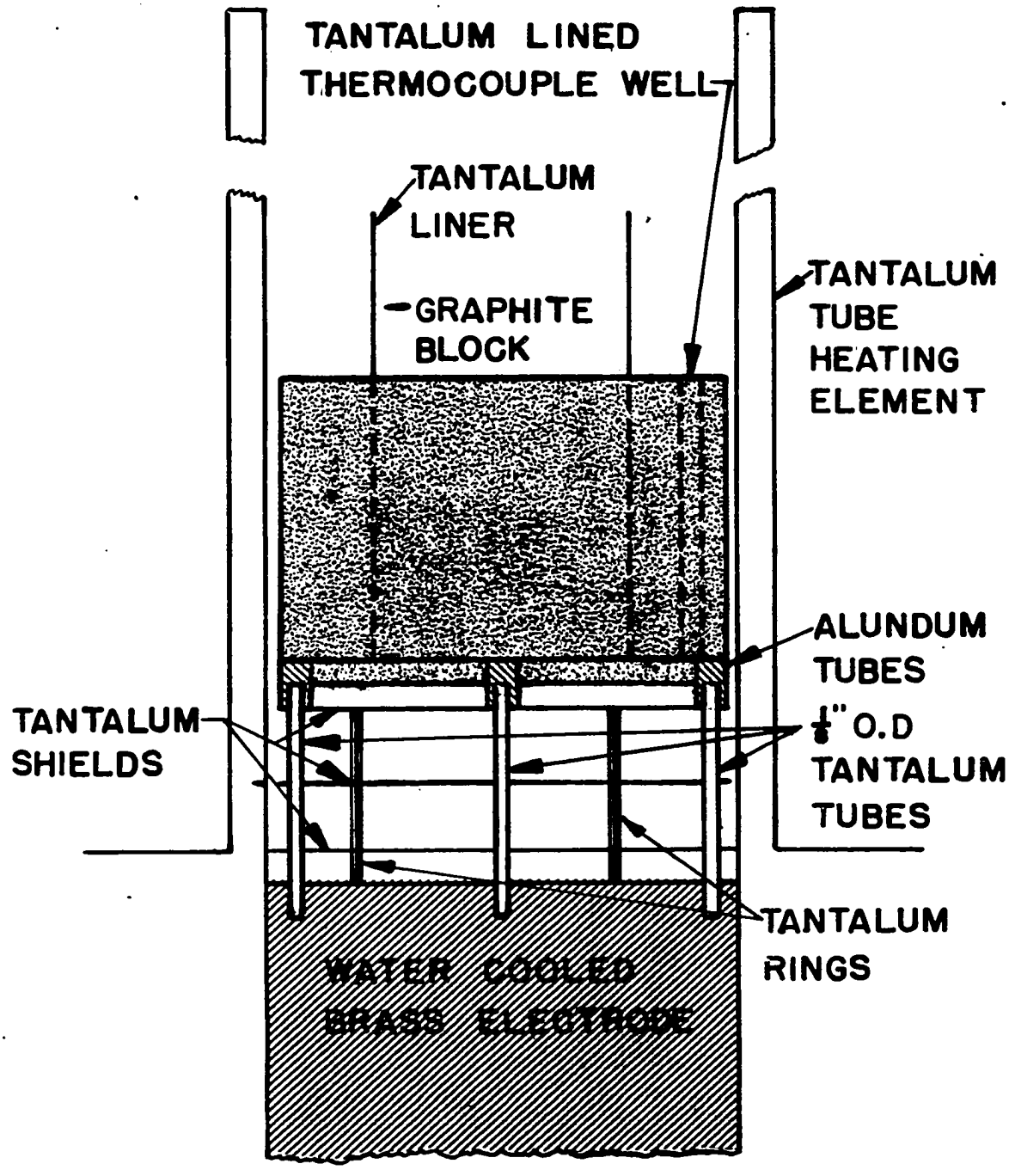

Figure 2. Heating zone of vacuum furnace

since its semi-conducting properties would make it a fairly good conductor at high temperatures. The block served to decrease the thermal gradients across the length of the sample and drastically improved the quality of the thermal analysis curves. The water-cooled brass cylinder shown in Figure 2 served as one electrode while the second electrode was the water-cooled main body of the furnace on which the shorter tantalum cylinder was fastened. Three molybdenum cylinders concentric to the heating element, separated by a distance of ¼", acted as shielding for the outside of the heating element. The top and bottom of the element were shielded by three round tantalum sheets. The lower three shields are shown in Figure 2. The thermocouples entered the thermocouple well through holes in the top shield. Although this method of introducing the thermocouples suffered from the disadvantage of exposing much of the thermocouple to the hot part of the furnace, it was thought to be desirable since it would decrease heat losses from the junction by conductivity. The tantalum liner shown in Figure 2 served a dual purpose. It protected the crucible containing the alloy from the carbon block and also shielded the crucible and decreased the thermal gradients across the length of the sample.

The power for heating the furnace was supplied by a step-down transformer with variable secondary voltage taps. The primary voltage was supplied by a powerstat operating on a 215

volt A.C. line. The voltage applied to the heating element was controlled by a second powerstat and was changed gradually by a motor attached to the variable contacts of the second powerstat. The heating and cooling rates were varied from 2° to 8° C per minute by changing either the primary voltage applied to the transformer or the secondary voltage taps of the transformer. In some samples the faster cooling rates were more effective in revealing the thermal breaks. About 2.7 kilowatts were required to attain a temperature of 1600° C in the sample.

Both differential and time-temperature thermal analysis were performed, since the transitions were not clearly defined in all the alloys by time-temperature thermal analysis. Thermal e.m.f's were determined both by a Bristol Company recording potentiometer and a Rubicon slide wire type potentiometer.

At least two heating and cooling curves were run with each sample with a precision of ± 5° C. However, the results of the study indicate an accuracy of ± 10° C for some alloys.

X-ray Diffraction Techniques

The structure assumed by the rare-earth alloys as functions of both composition and temperature were one of the main interests of this investigation. Room temperature x-ray diffraction patterns were taken using 57.3 and 114.6 mm North American Phillips Co. Debye-Scherrer cameras and copper K α

radiation. Originally, the samples were prepared from metal filings placed in a pyrex capillary in a dry box which could be evacuated and filled with helium. The capillaries were sealed in the dry box to retain a helium atmosphere and were annealed at 300-400° C overnight. The patterns obtained from these samples were very poor and contained impurity lines which were probably introduced by diffusion of moisture through the rubber gloves of the dry box.

Most of the room temperature X-ray diffraction samples used in the investigation were made employing a different method which gave better results. The alloy was rolled down to a thin sheet 0.007 inches thick. Small wires were cut from the sheet, scraped clean with a razor and placed in a thin-walled Pyrex capillary. The Pyrex capillary was evacuated to 3×10^{-7} mm of mercury and outgassed. It was then sealed off with this static vacuum and annealed at 200° C overnight. Higher annealing temperatures were used with lanthanum-yttrium, lanthanum-gadolinium and gadolinium-yttrium samples when the phase diagram for these systems had been determined, since annealing the samples at higher temperatures drastically improved the quality of the films. Cerium-yttrium, praseodymium-yttrium and neodymium-yttrium alloys were annealed at 200° C; this again was done to prevent quenching a high temperature form of these alloys.

The high temperature camera employed in this study was a

commercial camera originally described by Buerger, Buerger and Chesley (1943). The commercially available camera was modified by Hanak (1959) for studies of the high temperature structures of the pure rare-earth metals. The samples were prepared by a method which will be outlined below and was employed by Hanak (1959) in his studies of the pure rare-earth metals.

Wires made in the same way as has been described above were placed in a silica capillary with tungsten spacers to prevent contact of the wire sample with the capillary walls. The capillary was outgassed, evacuated to 3×10^{-7} mm of mercury and sealed off. These precautions made it possible to determine the structures of the alloys to temperatures of approximately 900° C.

The powder patterns of the alloys both at room and higher temperatures were of poorer quality than those of the pure metals. Back reflection lines were present only up to 400° C and in the La-Y, Ce-Y, Nd-Y and Pr-Y alloys the few back reflection lines present were broad and unresolved. This factor introduced larger errors into the determination of lattice constants.

The lattice constants of the alloys were determined by Cohen's least square method (1935-1936) programmed for an I.B.M. 650 electronic computor by Hanak (1959). The indexing portion of the program described by Hanak could not be used

since it required the prior knowledge of the lattice constants to an accuracy not possible with these alloys.

Microscopic Examination

Microscopic examination is a valuable method in the determination of the phase diagrams of metal systems. The main value of the method is to check pre-conceived ideas concerning the alloy system. Thus, it suffers the disadvantage of being subject to the interpretation of the investigator.

Several of the alloys were studied by this method. The sample was annealed at the desired temperature in a vacuum or inert gas atmosphere. The sample was mounted in Bakelite and polished with progressively finer mesh abrasives and finally with fine alundum powder to a mirror finish.

All of the metals and alloys studied were soft which resulted in a very disturbed surface from the initial rough abrasives. Several etching solutions were tried which only lightly etched the surface of the metal and retained the metallic luster of the sample. However, a light etch did not reveal the microstructure with the detail necessary to show the differences between phases which were as chemically similar as the phases encountered in this study.

It became clear that a more drastic etching solution would be necessary to define the microstructures of the alloys. Several strong etching solutions, concentrated nitric, 60 percent glacial acetic acid-40 percent nitric acid, 80 percent

nitric acid etc., were used but they always resulted in an inorganic film adhering to the surface of the sample and preventing examination of the metallic surface. In order to examine the metal surface after this strong etch, the film was removed by lightly polishing the sample with fine alundum powder. All the samples were treated in the same way and the microstructures of the alloys appear to be true representations of the alloy and not a result of the final polishing since they are consistent with the results of thermal analysis and the X-ray data.

RESULTS

The Lanthanum-Yttrium System

The phase diagram of the lanthanum-yttrium system derived from the results of this investigation is shown in Figure 3. An explanation of the structure notation employed throughout the thesis is shown in Table 2.

The results obtained by thermal analysis were generally reproducible to $\pm$ 5° C on heating and cooling, and in this system it was usually not necessary to run differential thermal analyses. Although the α - β transition in yttrium had not been experimentally observed at the time of this investigation, the thermal analysis results indicated a region of complete β solid solubility below the liquid-solid equilibrium region with an α - β transition in yttrium at 1490 $\pm$ 20° C. A peritectoid horizontal associated with the α La + α Y $\rightarrow$ β reaction was found at 895° C and 33 atomic percent yttrium. There is a eutectoid horizontal, $\beta \rightarrow \alpha$ La + α' La at 861° C and 10 atomic percent yttrium. The peritectoid horizontal, $\delta \rightarrow \alpha$ La + α Y occurs at 725 $\pm$ 25° C and 52 atomic percent yttrium. The δ phase, with a structure similar to the samarium structure determined by Daane et. al. (1954), exists from 50 $\pm$ 0.5 atomic percent yttrium to 55 $\pm$ 1.0 atomic percent yttrium at room temperature. The α Y region extends to 61 $\pm$ 1.5 atomic percent yttrium while the α La boundary occurs at 45 $\pm$ 1.5 atomic percent yttrium. The α La + α' La region is found up to

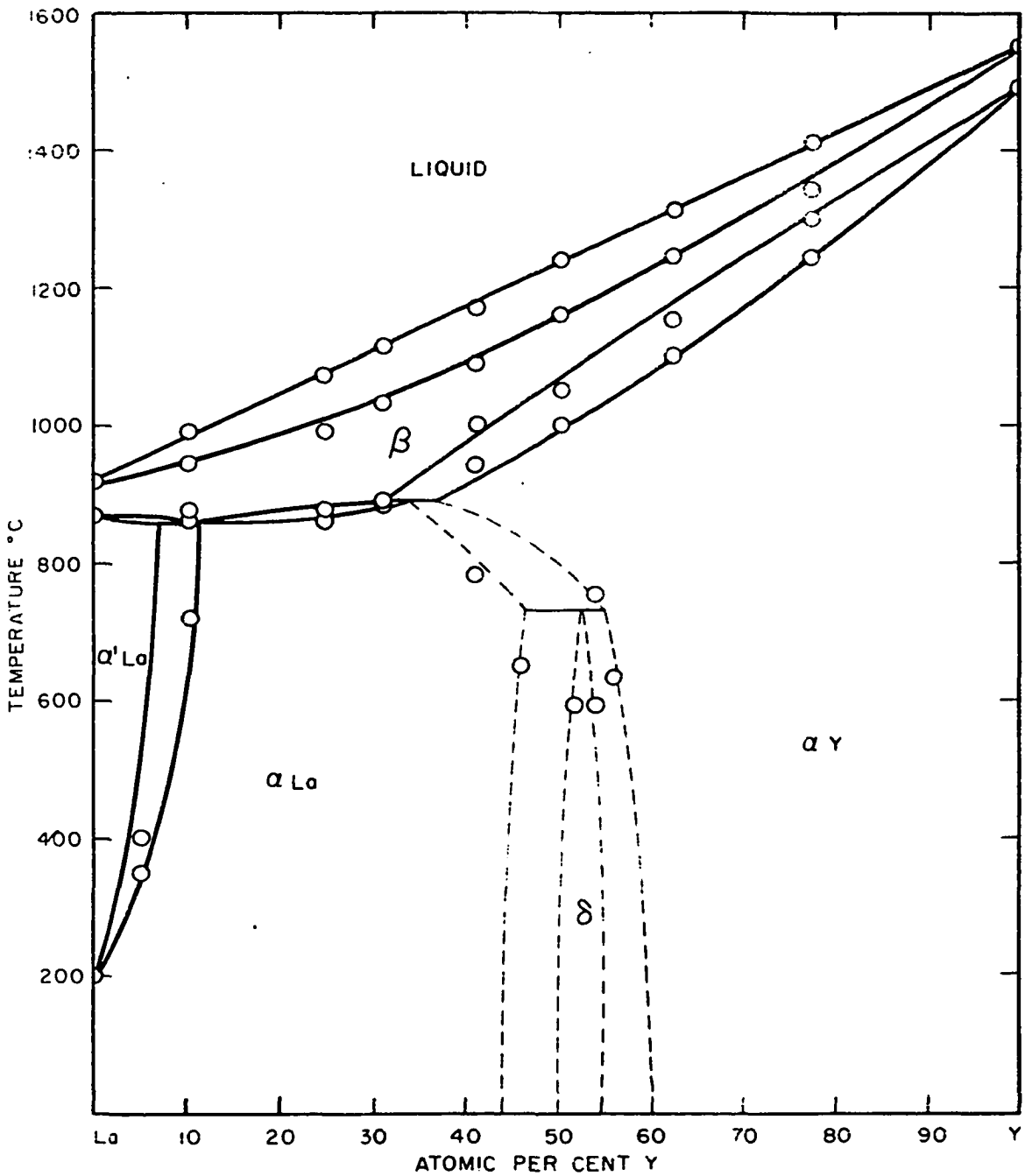

Figure 3. Phase diagram of the La-Y system

Table 2. Structure notation of the alloys

Notation	Structure
α La	h.c.p. ABAC stacking
α' La	f.c.c. ABC stacking
β La	b.c.c.
α Y	h.c.p. ABAB stacking
β Y	b.c.c.
α Gd	h.c.p. ABAB stacking
β Gd	b.c.c.
δ	ABCBCACAB stacking (samarium structure)

a maximum of 12 atomic percent yttrium. The results from which these conclusions are drawn will be discussed below.

The thermal analysis data are shown in small circles in Figure 3, and it can be seen that all the data lie on the boundaries drawn. The peritectoid horizontal was determined from the results of the thermal analysis of a 31.4 atomic percent yttrium alloy. This composition had been chosen on the basis of the extrapolation of the early thermal data which indicated that the peritectoid horizontal would be found at approximately 31 atomic percent yttrium. Thermal analysis of a 10.1 atomic percent yttrium alloy clearly indicated the

eutectoid horizontal $\beta \longrightarrow \alpha'$La + αLa at 861° C. The lengths of the horizontals were determined by extrapolation of the thermal data, except the low temperature peritectoid horizontal which was determined from high temperature X-ray data. The thermal analysis of some alloys gave results which could possibly be attributed to the low temperature αLa + $\delta \longrightarrow$ αLa + αY transition of the alloys, as in heating cycles of the 49.6 atomic percent yttrium alloy, a slight change in slope of the temperature versus time curve was noted at 710 $\pm$ 15° C. However, the changes were so small that they might have been caused by fluctuations in line voltages.

Transitions in the alloys concerned with changes in the stacking of the hexagonal close packed layers such as the αLa $\longrightarrow$ α'La and $\delta \longrightarrow$ αLa or αY could not be determined by thermal analysis. X-ray diffraction methods were the primary source of information for this region.

High temperature X-ray diffraction patterns were obtained for all the alloys over a range of temperatures from room temperature to approximately 875° C at 100° intervals. When a change in crystal structure occurred, the interval was reduced to 25° C which appeared to be the limit of reproducibility of the data obtained by this method. The high temperature X-ray results are shown as large circles in Figure 3.

The phase boundaries of the α'La + αLa equilibrium region were determined from the results of the study of a 5.0 atomic percent yttrium alloy and a 10.1 atomic percent yttrium

alloy. It was necessary to make an arbitrary choice for transformation temperatures since the alloys show the same hysteresis in this transformation as pure lanthanum. Once the α'La phase appears in an alloy, it disappears completely only after long annealing at 200° C. The α'La phase might have been stabilized by impurities because a face centered cubic impurity phase which had a smaller lattice constant than the metal, was obtained with many of the high temperature samples. This phase also has been observed by J. Hanak (1959) in his studies of the pure metals, and it is believed that the phase is a lower oxide of nitride of the rare earth. For the above reasons, it was assumed that the highest temperature obtained for a transformation on heating was probably the closest to the true equilibrium and these values were used. The X-ray diffraction lines of the metallic specimen in both the La-Gd and La-Y systems could be differentiated from the impurity lines at high temperatures since the metal lines were spotted due, probably, to the growth of large crystals. The 10.1 atomic percent yttrium alloy first showed lines attributed to the α'La structure at 720° C and did not transform completely to the α'La structure. At 860° C a pattern indexed as a mixture of the α'La and β structures was obtained. The 5.0 atomic percent yttrium alloy first showed the presence of the α'La structure at 350° C and completely transformed to the α'La structure at 400° C. The 15.0, 24.9 and 31.4 atomic percent yttrium alloys retained the αLa structure up to the

temperatures corresponding to the β transformation. The results obtained with the 12 atomic percent yttrium alloy were not consistent with the results obtained with the 10.1 and 5.0 atomic percent yttrium alloys. A complete transformation to face centered cubic occurred at 350° C and this phase disappeared only after overnight annealing at 200° C. It will be noted that this result cannot be explained on the basis of the phase diagram proposed here. However, pure lanthanum also shows a transformation to face centered cubic with hysteresis. The lattice constants obtained for some of the cubic alloys are shown in Table 3.

Table 3. Lattice constants of cubic alloys

Temperature °C	Atomic percent yttrium	a(A)	Structure
350	5.0	5.29 ± 0.01 A	f.c.c.
400	5.0	5.321 ± 0.003 A	f.c.c.
450	5.0	5.303 ± 0.002 A	f.c.c.
500	5.0	5.322 ± 0.006 A	f.c.c.
585	5.0	5.325 ± 0.008 A	f.c.c.
695	5.0	5.325 ± 0.002 A	f.c.c.
646	10.1	5.327 ± 0.008 A	f.c.c.
738	10.1	5.324 ± 0.007 A	f.c.c.
853	15.0	4.236 ± 0.005 A	b.c.c.
904	24.9	4.23 ± 0.01 A	b.c.c.

Table 4. X-ray diffraction data of 50.2 atomic percent yttrium alloy at 775° C

hkl α La	hkl α Y	$\sin^2\theta$ observed	$\sin^2\theta$ [a] calculated α La	$\sin^2\theta$ [b] calculated α Y
10,0	10,0	0.0582	0.0570	0.0581
10,1	--	0.0657	0.0610	--
00,4	00,2	0.0688	0.0651	0.0676
10,2	10,1	0.0744	0.0732	0.0750
10,4	--	0.1218	0.1220	--
--	10,2	0.1262	--	0.1257
11,0	11,0	0.1714	0.1709	0.1747
10,6	--	0.2041	0.2033	--
--	10,3	0.2098	--	0.2102
11,4	--	0.2397	0.2359	--
--	11,2	0.2447	--	0.2420
00,8	--	0.2631	0.2602	--
--	00,4	0.2691	--	0.2704
20,6	--	0.3775	0.3749	--

[a]Calculated using lattice constants, a = 3.73 ± 0.02 A and c = 12.09 ± 0.08 A.

[b]Calculated using lattice constants, a = 3.692 ± 0.002 A and c = 5.930 ± 0.003 A.

The 41.6 atomic percent yttrium alloy retained the α La structure to 784 ± 25° C where a pattern was obtained which at first appeared to be an α La pattern. However, closer inspection revealed that it was a two phase pattern in which the lines of the α La structure which coincided with α Y

lines were broad at low angles and split into two lines at higher values of θ. The two phase pattern was more evident in the 50.2 atomic percent yttrium alloy at 775° C since the lines were split at even lower values of θ. Table 4 shows the results of indexing this pattern with the lattice constants, α La phase a = 3.73 ± 0.02 A, c = 12.09 ± 0.08 A, α Y phase, a = 3.692 ± 0.002 A, c = 5.930 ± 0.003 A.

The patterns obtained with this alloy were complex at room temperature. Many of the lines could be indexed as α La lines but a large number of lines did not fit this indexing or an α Y structure. The pattern was indexed as a structure analogous to the samarium structure, δ phase, with hexagonal lattice constants, a = 3.687 ± 0.007 A, c = 26.76 ± 0.02 A. This structure can also be indexed as rhombohedral but since the original indexing was based on the hexagonal unit cell and also to make comparisons with the hexagonal α Y and α La structures of the other alloys easier, the hexagonal lattice constants of this δ phase will be used. The phase was also encountered in the 52.1 and 54.0 atomic percent yttrium alloy with lattice constants, a = 3.698 ± 0.006 A, c = 26.70 ± 0.05 A, and a = 3.697 ± 0.004 A, c = 26.86 ± 0.03 A, respectively. Table 5 shows the observed and calculated values of $\sin^2 \theta$ for the 52.1 atomic percent yttrium alloy. The patterns of the 46.0, 49.0, 55.9, and 59.0 atomic percent yttrium alloys were indexed as two phase patterns. The patterns obtained for the 46.0 and 49.0 atomic percent yttrium alloys were

Table 5. X-ray diffraction data of 52.05 atomic percent yttrium alloy

Int.	hkl	$\sin^2\theta$ observed	$\sin^2\theta$ [a] calculated	$\Delta \sin^2\theta$ observed-calculated
S	00,9	0.0686	0.0675	0.0010
vvw	10,4	0.0728	0.0712	0.0015
w	10,5	0.0795	0.0787	0.0007
vvw	10,7	0.0958	0.0987	-0.0029
vvw	10,8	0.1112	0.1112	-0.0000
vvw	10,10	0.1413	0.1412	0.0000
w	11,0	0.1744	0.1737	0.0006
w	10,13	0.2009	0.1987	0.0021
w	10,14	0.2216	0.2213	0.0002
m	11,9	0.2422	0.2412	0.0009
m	00,18	0.2711	0.2701	0.0010
vvw	20,13	0.3677	0.3725	0.0052
vvw	10,19	0.3677	0.3588	-0.0011
vvw	10,20	0.3940	0.3913	0.0026
vvw	20,14	0.3940	0.3950	-0.0010
vw	21,4	0.4214	0.4187	0.0027
w	11,18	0.4448	0.4438	0.0009
vw	10,23	0.4997	0.4989	0.0007
vvw	21,13	0.5493	0.5462	0.0030
vvw	20,20	0.5667	0.5650	0.0015
vvw	30,9	0.5882	0.5887	-0.0005
vvw	00,27	0.6104	0.6077	0.0027
vvw	20,22	0.6350	0.6351	-0.0001
vvw	31,4	0.7647	0.7648	-0.0002
vvw	11,27	0.7793	0.7801	-0.0008
vvw	30,18	0.7908	0.7899	+0.0008

[a]Calculated using lattice constants, a = 3.699 $\pm$ 0.007 A and c = 26.70 $\pm$ 0.05 A.

identical, as were the patterns of the 55.9 and 59.0 atomic percent yttrium alloys. The 46.0 atomic percent yttrium alloy was indexed as a mixture of the α La and δ phase, while that of the 55.9 atomic percent yttrium alloy as a two phase δ + α Y alloy. The observed and calculated $\sin^2\theta$ for the 46.0 and 55.9 atomic percent yttrium alloy are shown in Tables 6 and 7, respectively.

The 46.0 atomic percent yttrium alloy transformed to the α La structure at 660° C; the 52.1 atomic percent yttrium alloy first showed lines of the α La structure at 588° C; the 54.0 atomic percent yttrium alloy showed a transformation from δ to δ + α Y at 590° C and to α Y at 750° C; the 55.9 atomic percent yttrium alloy transformed from α Y + δ to the α Y structure at 633° C. The room temperature boundaries could not be determined with great accuracy from the X-ray data but it is believed that the boundaries shown in Figure 3 are accurate to $\pm$ 1.5 atomic percent yttrium.

The 62.4 and 77.5 atomic percent yttrium alloys retained the α Y structure from room temperature to 860° C. This temperature was the limiting temperature for obtaining readable X-ray films with these samples.

The lack of resolution of back reflection lines inherent in this binary alloy system made it impossible to evaluate the lattice constants with the desired accuracy. The average standard deviation was about $\pm$ 0.005 A. Figure 4 illustrates the variation of the lattice constant, a, versus composition for

Table 6. X-ray diffraction data of 46.0 atomic percent yttrium alloy

hkl αLa structure	hkl Sm structure	$\sin^2\theta$ observed	$\sin^2\theta$ [a] calculated La structure	$\sin^2\theta$ [b] calculated Sm structure
00,4	00,9	0.0677	0.0669	0.0673
--	10,4	0.0717	--	0.7036
10,2	--	0.0752	0.0745	--
--	10,5	0.0801	--	0.0778
10,3	10,7	0.0973	0.0954	0.0978
--	10,8	0.1118	--	0.1103
--	10,10	0.1403	--	0.1402
00,6	--	0.1511	0.1505	--
10,5	--	0.1623	0.1623	--
11,0	11,0	0.1734	0.1733	0.1711
--	10,13	0.1989	--	0.1976
10,6	--	0.2073	0.2082	--
--	10,14	0.2206	--	0.2201
11,4	11,9	0.2402	0.2402	0.2385
10,7	--	0.2612	0.2626	--
20,4	10,17	0.2998	0.2980	0.2975
--	10,19	0.3586	--	0.3574
--	20,13	0.3687	--	0.3687
10,9	10,20	0.3904	0.3964	0.3898
00,10	--	0.4174	0.4180	--
11,8	11,18	0.4409	0.4409	0.4407
--	10,22	0.4597	--	0.4597
21,4	--	0.4720	0.4714	--
20,8	10,23	0.4966	0.4987	0.4971
--	20,19	0.5300	--	0.5284
--	20,20	0.5595	--	0.5609
10,11	--	0.5650	0.5636	--

[a]Calculated using lattice constants, a = 3.703 ± 0.007 A and c = 11.923 ± 0.01 A.

[b]Calculated using lattice constants, a = 3.727 ± 0.003 A and c = 26.73 ± 0.02 A.

Table 6. (Continued)

hkl α La structure	hkl Sm structure	$\sin^2\theta$ observed	$\sin^2\theta$ [a] calculated La structure	$\sin^2\theta$ [b] calculated Sm structure
30,4	30,9	0.5854	0.5870	0.5808
00,12	00,27	0.6044	0.6019	0.6065
--	20,22	0.6304	--	0.6308
30,6	20,23	0.6692	0.6706	0.6683
22,4	10,29	0.7581	0.7590	0.7554
--	11,27	0.7759	--	0.7763
30,8	20,26	0.7865	0.7863	0.7892
--	21,22	0.8020	--	0.8006
00,14	--	0.8165	0.8179	--
22,6	--	0.8450	0.8425	--
--	10,31	0.8545	--	0.8551
31,6	31,14	0.9028	0.9002	0.9031
22,8	31,16	0.9558	0.9593	0.9529

the alloys, while Figure 5 illustrates the dependence of 2c/no. of atoms per unit cell, c, on composition. This value is twice the distance between two hexagonal close packed planes, which reduces to the c axis for the ABAB hexagonal structures. Figure 6 shows the dependence of density on composition.

The Lanthanum-Gadolinium System

The phase diagram proposed for the lanthanum-gadolinium system is shown in Figure 7. It can be seen that this phase

Table 7. X-ray diffraction data of 55.9 atomic percent yttrium alloy

hkl αY structure	hkl Sm structure	$\sin^2\theta$ observed	$\sin^2\theta$ [a] calculated Y structure	$\sin^2\theta$ [b] calculated Sm structure
10,0	10,1	0.0598	0.0577	0.0585
00,2	00,9	0.0689	0.0690	0.0674
10,1	--	0.0759	0.0750	--
--	10,5	0.0801	--	0.0785
--	10,7	0.0989	--	0.0985
--	10,8	0.1123	--	0.1110
10,2	--	0.1281	0.1267	--
--	10,10	0.1426	--	0.1410
11,0	11,0	0.1746	0.1732	0.1732
--	10,13	0.1997	--	0.1985
10,3	--	0.2136	0.2130	--
--	10,14	0.2211	--	0.2210
11,2	11,9	0.2426	0.2422	0.2407
20,1	20,4	0.2506	0.2482	0.2443
--	00,18	0.2716	--	0.2698
00,4	--	0.2759	0.2760	--
20,2	10,17	0.3020	0.3000	0.2985
10,4	--	0.3352	0.3337	--
--	10,19	0.3588	--	0.3584
--	20,13	0.3736	--	0.3718
20,3	--	0.3876	0.3862	--
--	20,14	0.3953	--	0.3942
21,0	21,2	0.4070	0.4043	0.4076
21,1	--	0.4224	0.4215	--
--	20,16	0.4463	--	0.4442
--	10,22	0.4635	--	0.4609
21,2	--	0.4748	0.4733	--

[a]Calculated using lattice constants, a = 3.704 ± 0.003 A and c = 5.869 ± 0.004 A.

[b]Calculated using lattice constants a = 3.703 ± 0.003 A and c = 26.71 ± 0.02 A.

Table 7. (Continued)

hkl αY structure	hkl Sm structure	$\sin^2\theta$ observed	$\sin^2\theta$ [a] calculated Y structure	$\sin^2\theta$ [b] calculated Sm structure
10,5	--	0.4896	0.4890	--
--	10,23	0.5012	--	0.4984
20,4	21,11	0.5099	0.5070	0.5050
30,0	30,0	0.5221	0.5198	0.5198
--	21,13	0.5467	--	0.5450
21,3	--	0.5605	0.5595	--
--	21,14	0.5683	--	0.5675
30,2	30,9	0.5887	0.5888	0.5872
--	00,27	0.6083	--	0.6072
00,6	--	0.6216	0.6210	--
--	20,22	0.6376	--	0.6341
20,5	--	0.6606	0.6622	--
10,6	--	0.6783	0.6787	--
22,0	22,0	0.6919	0.6919	0.6919
22,2	22,9	0.7596	0.7609	0.7592
22,2	22,9	0.7652	0.7646	0.7630
11,6	30,18	0.7910	0.7929	0.7883
21,5	31,10	0.8330	0.8341	0.8328
00,7	21,23	0.8449	0.8437	0.8435
10,7	--	0.8995	0.9014	--
--	10,32	0.9093	--	0.9092
--	22,18	0.9630	--	0.9613

diagram is very similar to that of the lanthanum-yttrium system indicating that the β form of gadolinium is also body centered cubic.

The high temperature phase boundaries in this system were determined by differential thermal analysis in most alloys

Figure 4. a vs. composition of the La-Y system

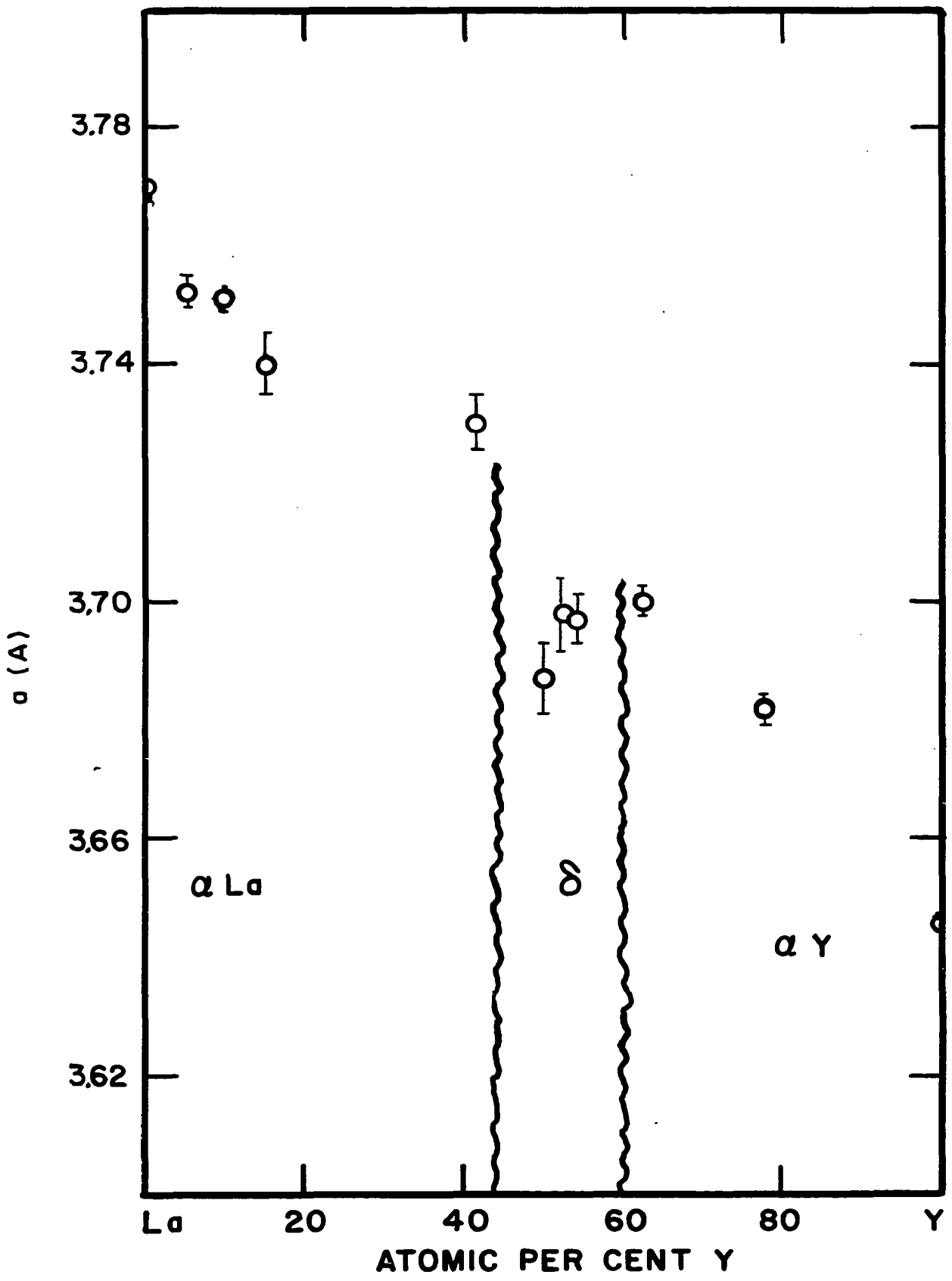
3.78
3.74
3.70
3.66
3.62
a (A)
α La
δ
α Y
La
20
40
60
80
Y
ATOMIC PER CENT Y

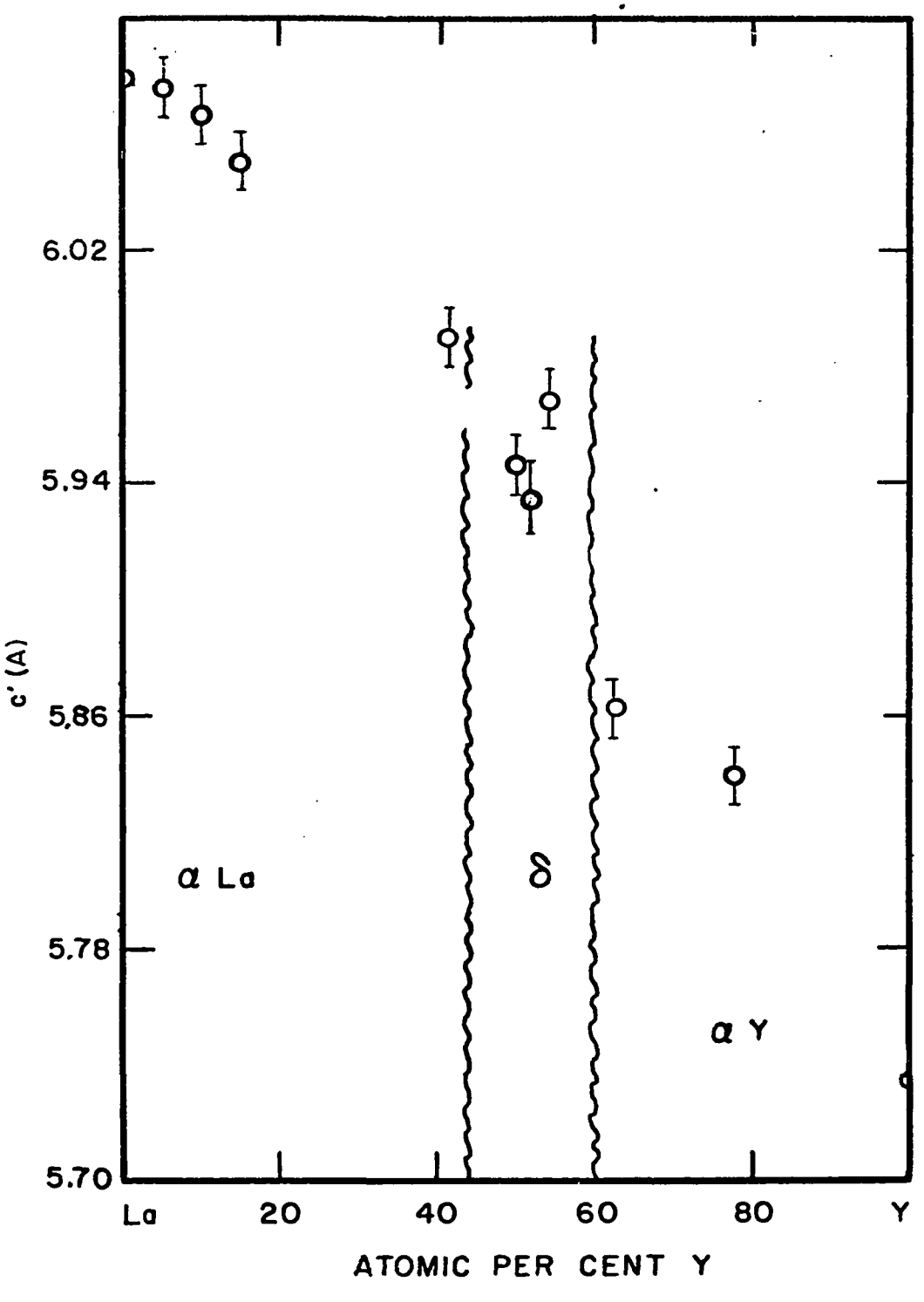

Figure 5. c' vs. composition of the La-Y system

Figure 6. Density vs. composition of the La-Y system

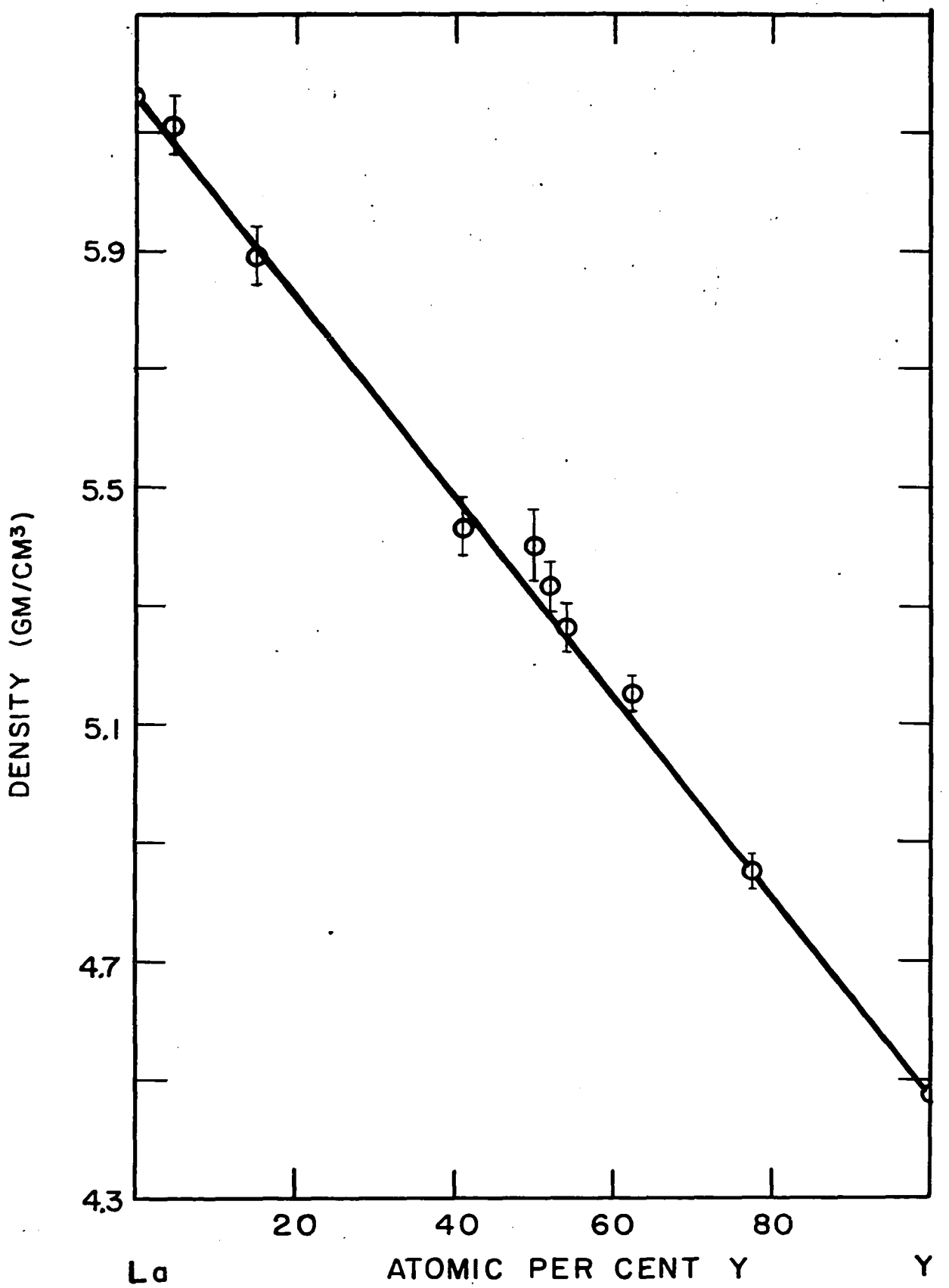
DENSITY (GM/CM³)
5.9
5.5
5.1
4.7
4.3
20
40
60
80
La
ATOMIC PER CENT Y
Y

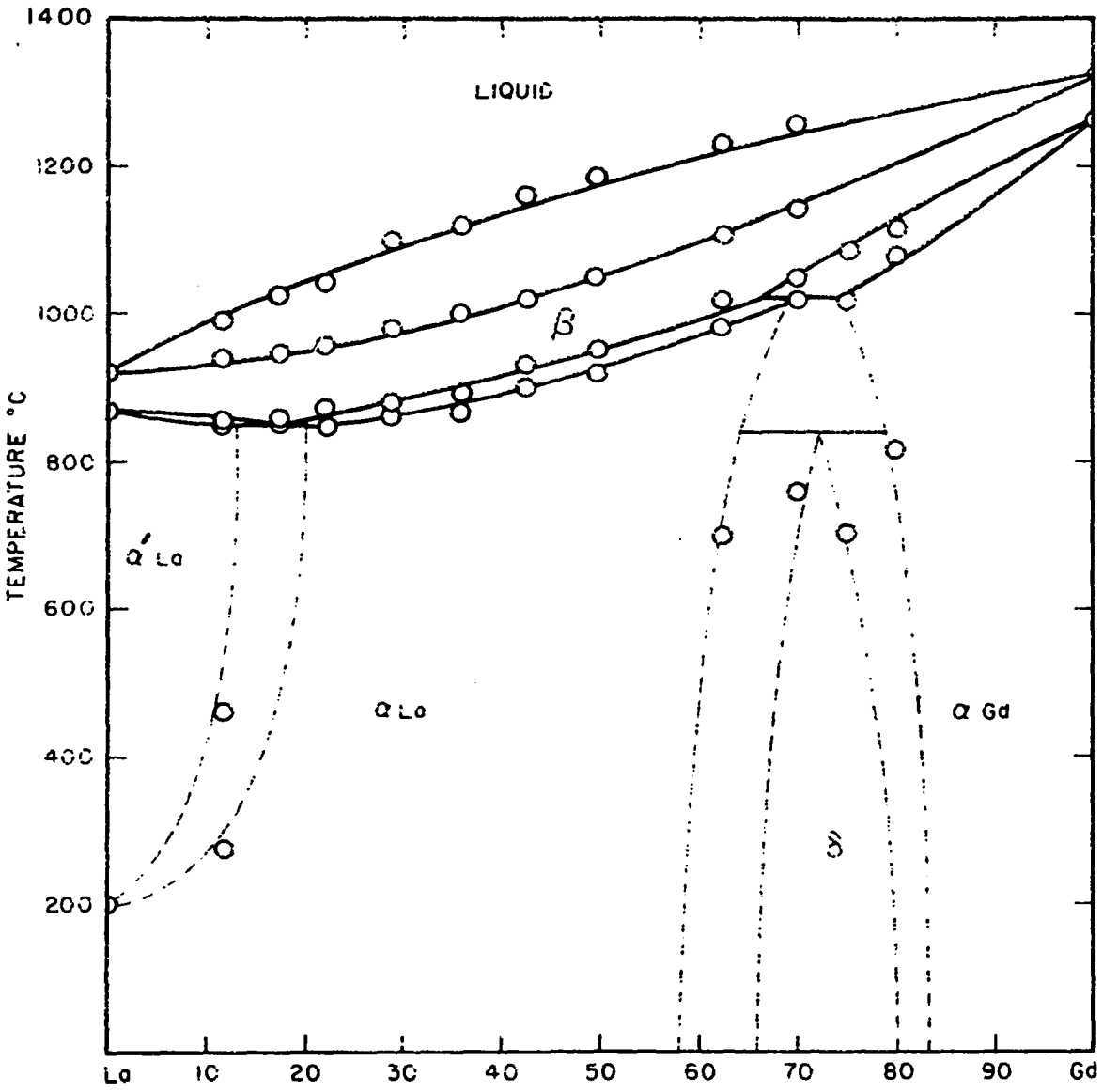

Figure 7. Phase diagram of the La-Gd system

since the breaks on a time-temperature thermal analysis were not clear. Also the reproducibility of the results is much poorer than those of the lanthanum-yttrium system. The thermal analysis results are shown as small circles in Figure 7.

The high temperature X-ray patterns were taken over temperature intervals of 100° C except when a transformation occurred and the interval was reduced to 25° C as in the lanthanum-yttrium system.

A region of complete β solid solution exists above the α'La $\rightarrow \beta$ and α Gd $\rightarrow \beta$ transitions. The peritectoid horizontal, α La + α Gd $\rightarrow \beta$ was found at 1024° C and 70 atomic percent gadolinium. The eutectoid horizontal, associated with $\beta \rightarrow \alpha'$La + αLa reaction occurred at 853° C and 15 atomic percent gadolinium. Again, as in the La-Y system, the lengths of the horizontals were determined by extrapolation of the thermal data and X-ray data.

The low temperature transitions again had to be determined by high temperature X-ray diffraction. A mixture of the α and α' phases was found in an 11.7 atomic percent gadolinium alloy at 268° C and a pattern that could be completely indexed as face centered cubic was first obtained at 460° C. The alloy containing 17.2 atomic percent gadolinium gave anomalous results for the $\alpha - \alpha'$ transformation, similar to those obtained with 12 atomic percent yttrium alloy described earlier. Most of the high temperature X-ray samples contained the α'La phase even at room temperature; in fact, some

samples showed only the α'La structure after prolonged annealing at 200° C. It is possible that this phase is impurity stabilized and that this caused the anomalous behavior of this alloy. However, the explanation might be a kinetic effect. It appears that further studies of the α - α'La structure will be necessary to resolve the anomaly.

The alloys containing 22.2, 28.8, 35.3, 42.5 and 49.6 atomic percent gadolinium showed no structure transformations below the $\alpha \rightarrow \beta$ transformation. This indicated that the α' region did not extend as far as 22.2 atomic percent gadolinium.

The 58.4, 62.5 and 64.9 atomic percent gadolinium alloys were a mixture of two phases δ + α La, at room temperature. The lattice constants and observed and calculated $\sin^2\theta$'s for the 64.9 atomic percent gadolinium alloy are shown in Table 8. The 62.5 atomic percent gadolinium alloy transformed to the α La structure at 700° C while the 64.9 atomic percent gadolinium alloy retained the mixed α La + δ structure to 845° C where there was a distinct change in pattern. The pattern contained very few spotted metal lines, but it appeared to be composed of a mixture of α Gd and α La lines. The pattern contained too few lines to determine this unequivocably, due to the high temperature necessary to effect this transformation.

The patterns obtained for the 69.9, 74.5 and 79.6 atomic

Table 8. X-ray diffraction data of 64.9 atomic percent gadolinium alloy

hkl La structure	hkl Sm structure	$\sin^2\theta$ observed	$\sin^2\theta$ [a] calculated La structure	$\sin^2\theta$ [b] calculated Sm structure
10,1	--	0.0662	0.0628	--
00,4	00,9	0.0692	0.0674	0.0682
--	10,4	0.0731	--	0.0725
10,2	--	0.0769	0.0755	--
--	10,5	0.0817	--	0.0800
10,3	--	0.0959	0.0966	--
--	10,7	0.0989	--	0.1003
10,5	--	0.1653	0.1640	--
--	11,0	0.1791	--	0.1770
11,2	--	0.1906	0.1928	--
10,6	--	0.2137	0.2104	--
--	10,14	0.2253	--	0.2241
--	11,9	0.2468	--	0.2453
--	00,18	0.2750	--	0.2729
20,6	20,13	0.3829	0.3864	0.3784
--	10,20	0.3914	--	0.3960
10,9	20,14	0.4025	0.4000	0.4012
00,10	--	0.4205	0.4215	--
21,2	21,4	0.4292	0.4275	0.4266
--	11,18	0.4517	--	0.4500
10,10	20,17	0.4781	0.4801	0.4790
--	30,0	0.5326	--	0.5311
11,10	30,9	0.6000	0.5975	0.5994
21,7	00,27	0.6162	0.6172	0.6141
31,2	22,9	0.7774	0.7782	0.7751
--	$11,27\alpha_1$	0.7903	--	0.7898
--	$11,27\alpha_2$	0.7946	--	0.7938
$30,8\alpha_1$	--	0.7955	0.7964	--
$30,8\alpha_2$	--	0.8009	0.8004	--
10,14	$20,28\alpha_1$	0.8911	0.8833	0.8950
--	$22,18\alpha_1$	0.9790	--	0.9795

[a] Calculated using lattice constants, a = 3.675 ± 0.005 A and c = 11.874 ± 0.007 A.

[b] Calculated using lattice constants, a = 3.664 ± 0.003 A and c = 26.56 ± 0.04 A.

Table 9. X-ray diffraction data of 69.92 atomic percent gadolinium alloy

Int.	hkl	$\sin^2\theta$ observed	$\sin^2\theta$ [a] calculated
s	00,9	0.0698	0.0686
vw	10,4	0.0734	0.0724
w	10,5	0.0813	0.0801
vvw	10,7	0.0951	0.1004
vvw	10,8	0.1149	0.1131
vvw	10,10	0.1452	0.1436
m-	11,0	0.1783	0.1767
m	10,13	0.2030	0.2021
m	10,14	0.2259	0.2250
vvw	20,2	0.2399	0.2390
m	11,9	0.2474	0.2454
vvw	20,5	0.2588	0.2568
m	00,18	0.2758	0.2745
m	10,16	0.2758	0.2758
vvw	10,17	0.3051	0.3038
vw	20,13	0.3812	0.3789
vw	20,14	0.4034	0.4017
vvw	21,4	0.4274	0.4260
vvw	21,5	0.4343	0.4336
m	11,18	0.4526	0.4513
w	10,22	0.4700	0.4690
vvw	20,17	0.4804	0.4806
vvw	10,23	0.5075	0.5072
vvw	21,13	0.5562	0.5556
vvw	21,14	0.5796	0.5785
vw	30,9	0.6010	0.5989
vw	00,27	0.6189	0.6177
vvw	10,26	0.6341	0.6317
vvw	20,22	0.6466	0.6458
vvw	22,9 α_1	0.7749	0.7744

[a]Calculated using lattice constants, a = 3.667 $\pm$ 0.001 A and c = 26.482 $\pm$ 0.007 A.

Table 9. (Continued)

Int.	hkl	$\sin^2\theta$ observed	$\sin^2\theta$ [a] calculated
vvw	$22,9\alpha_2$	0.7778	0.7783
vvw	$11,27\alpha_1$	0.7943	0.7932
vvw	$11,27\alpha_2$	0.7971	0.7971
vvw	$30,18\alpha_1$	0.8050	0.8035
vvw	$30,18\alpha_2$	0.8075	0.8075
vvw	$21,22\alpha_1$	0.8217	0.8212
vvw	$21,23\alpha_1$	0.8600	0.8593
vvw	$21,23\alpha_2$	0.8642	0.8636
vvw	$10,31\alpha_1$	0.8723	0.8718
vvw	$10,31\alpha_2$	0.8765	0.8761
vvw	$10,32\alpha_1$	0.9238	0.9251
vvw	$10,32\alpha_2$	0.9306	0.9297
vvw	$22,18\alpha_1$	0.9802	0.9800
vvw	$22,18\alpha_2$	0.9847	0.9849

percent gadolinium alloys gave patterns which were indexed as a single δ phase. Table 9 is a compilation of the observed and calculated $\sin^2\theta$'s for the 69.9 atomic percent gadolinium alloy. As can be seen in Table 9, the agreement between the observed and calculated $\sin^2\theta$'s is much better since the patterns contained resolved back reflections and the lattice constants could be determined with greater accuracy. An alloy containing 81.8 atomic percent gadolinium was indexed as a mixture of the δ and α Gd phases. Table 10 shows the result of this indexing. Figures 8, 9 and 10 show the variation in

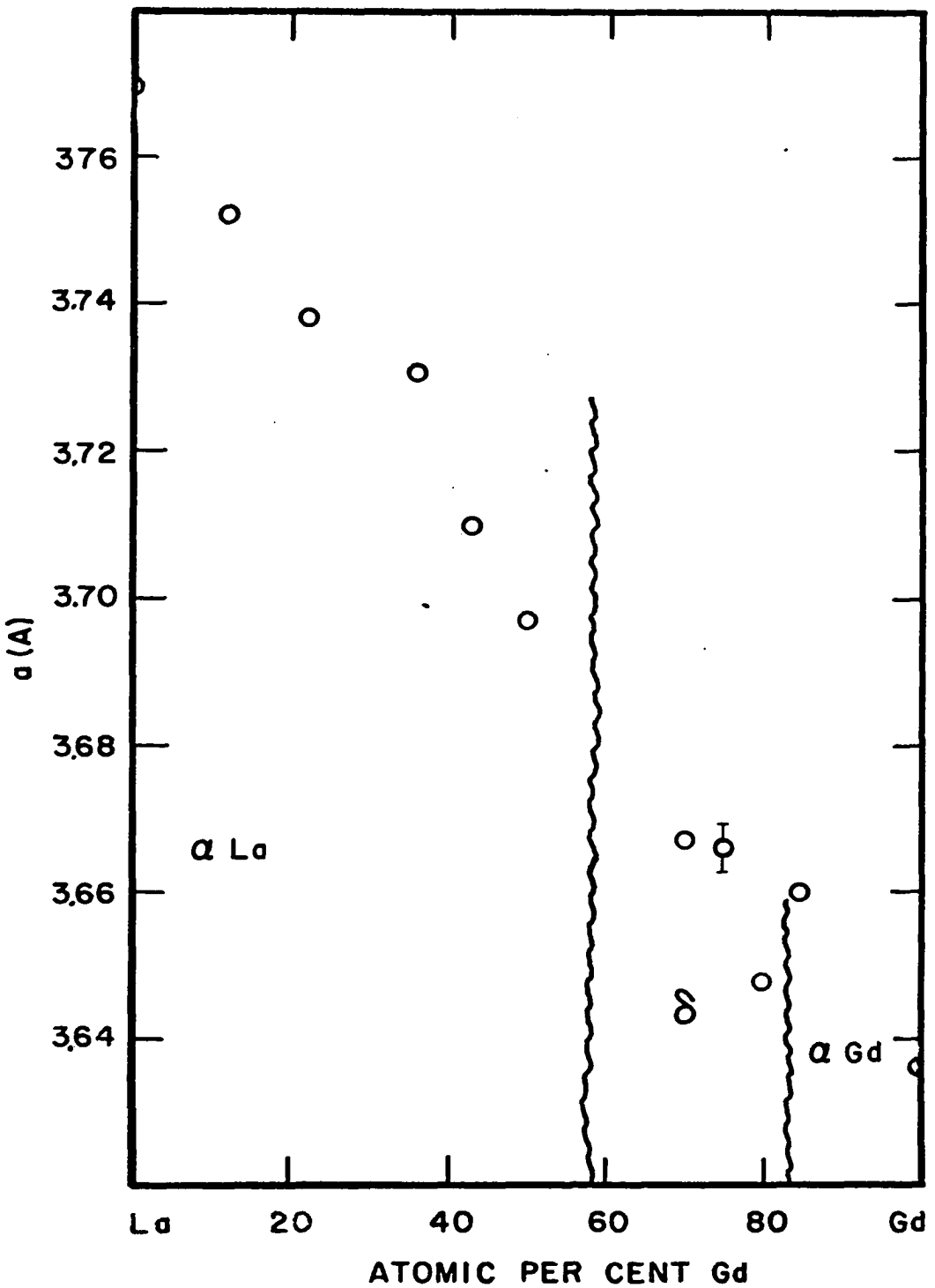

Figure 8. a vs. composition of the La-Gd system

Figure 9. c' vs. composition of the La-Gd system

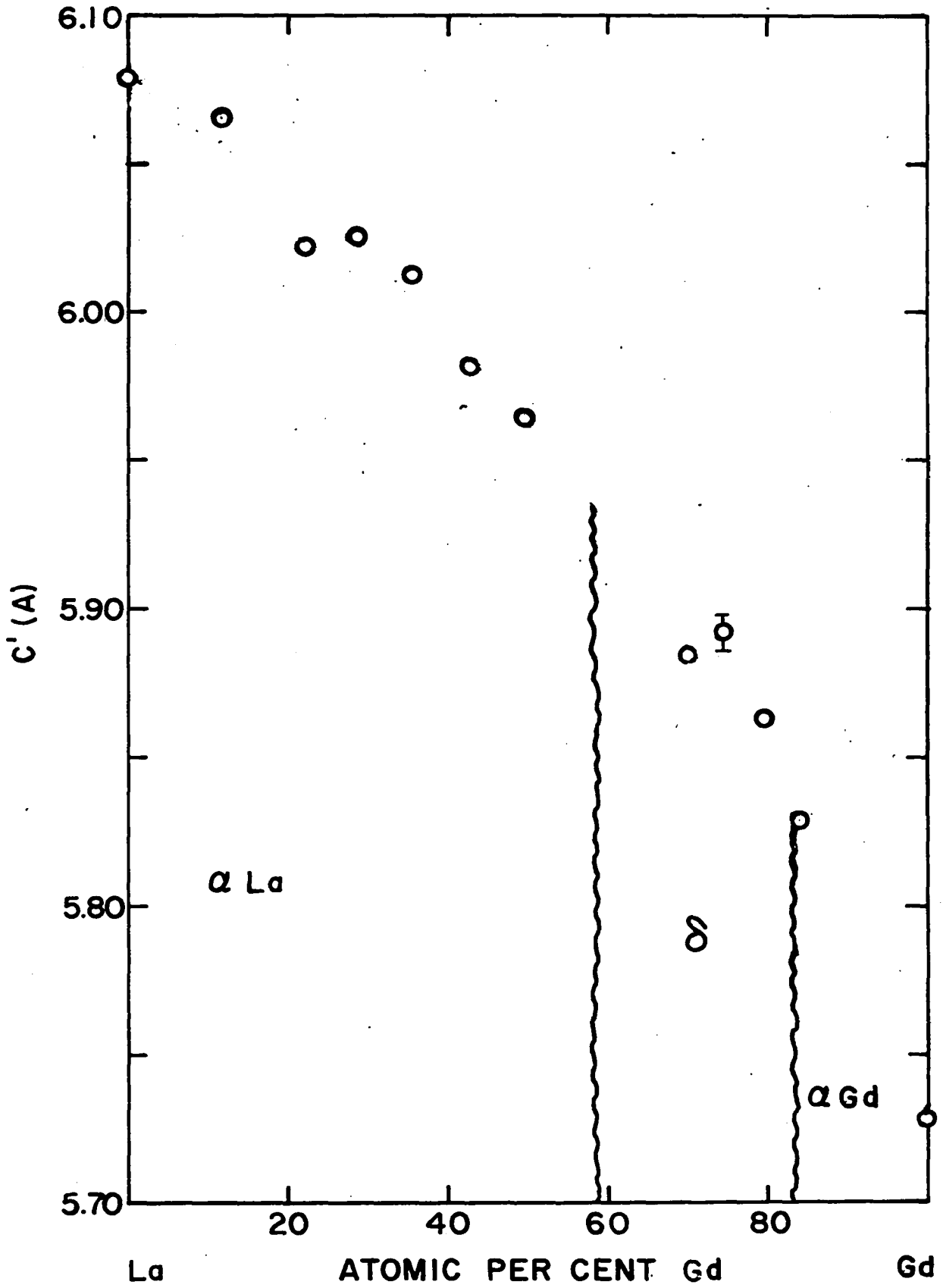
6.10
6.00
5.90
5.80
5.70
C' (A)
α La
δ
α Gd
20
40
60
80
La
ATOMIC PER CENT Gd
Gd

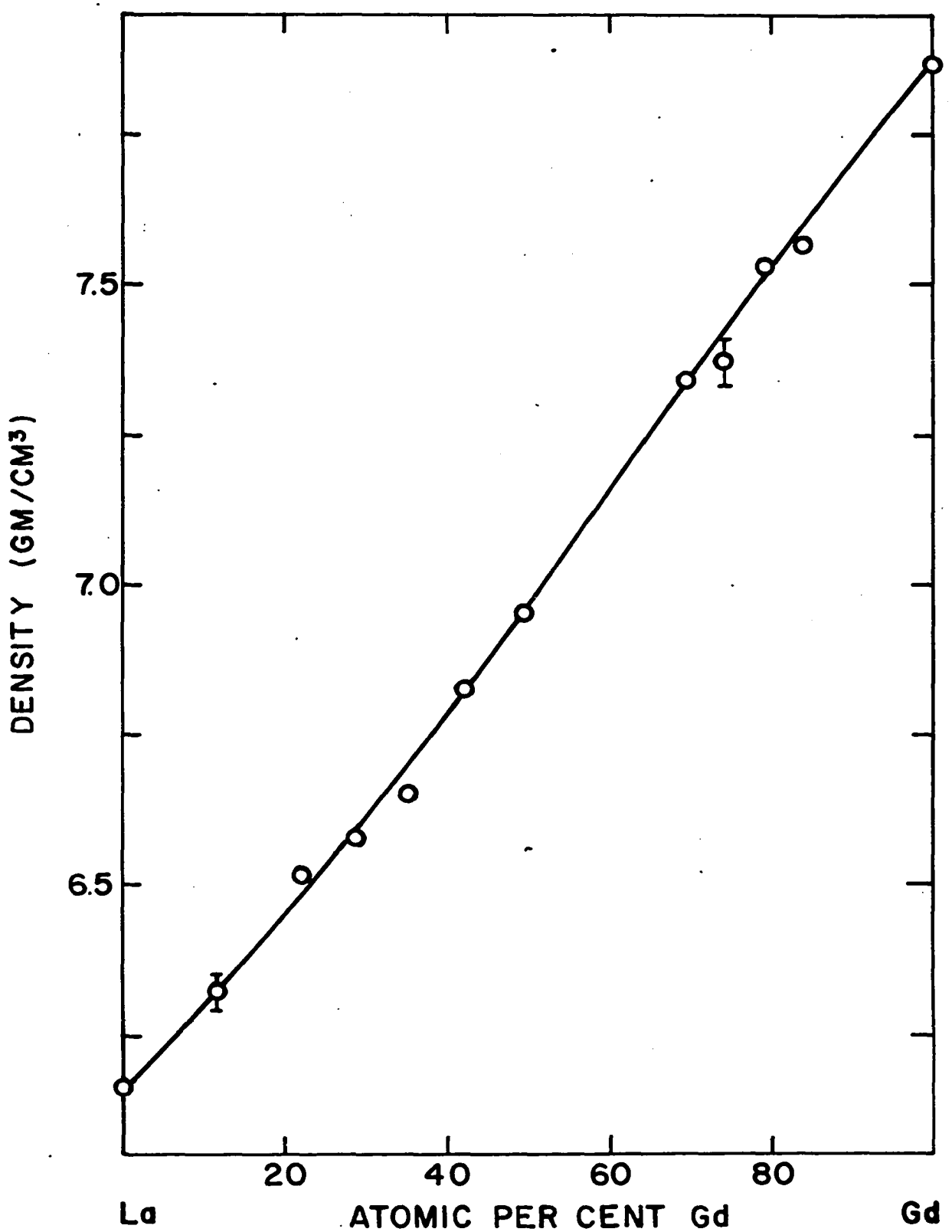

Figure 10. Density vs. composition of the La-Gd system

Table 10. X-ray diffraction data of 81.81 atomic percent gadolinium alloy

hkl Gd structure	hkl Sm structure	$\sin^2\theta$ observed	$\sin^2\theta$ [a] calculated Gd structure	$\sin^2\theta$ [b] calculated Sm structure
00,2	00,9	0.0700	0.0698	0.0692
--	10,4	0.0736	--	0.0732
10,1	--	0.0773	0.0767	--
--	10,5	0.0811	--	0.0809
10,2	--	0.1287	0.1297	--
00,3	10,10	0.1524	0.1571	0.1451
11,0	11,0	0.1780	0.1774	0.1787
--	10,13	0.2031	--	0.2041
10,3	--	0.2166	0.2162	--
--	10,14	0.2272	--	0.2272
11,2	11,9	0.2475	0.2472	0.2479
--	20,5	0.2629	--	0.2596
00,4	00,18	0.2784	0.2793	0.2771
10,4	--	0.3385	0.3385	--
--	10,19	0.3724	--	0.3683
20,3	10,20	0.3940	0.3937	0.4016
21,1	21,4	0.4311	0.4316	0.4306
11,4	11,18	0.4564	0.4568	0.4558
--	10,22	0.4783	--	0.4735
10,5	--	0.4949	0.4956	--
--	10,23	0.5123	--	0.5120
21,3	21,13	0.5694	0.5711	0.5615
30,2	30,9	0.6025	0.6021	0.6054
--	10,25	0.6025	--	0.5941
00,6	00,27	0.6258	0.6285	0.6235
--	20,25	0.7683	--	0.7715
--	20,25	0.7724	--	0.7753
--	11,27	0.8021	--	0.8008
30,4	30,18	0.8134	0.8103	0.8116
--	21,22	0.8331	--	0.8295
21,5	--	0.8494	0.8498	--

[a]Calculated using lattice constants, a = 3.660 ± 0.002 A and c = 5.83 ± 0.003 A.

[b]Calculated using lattice constants, a = 3.647 ± 0.002 A and c = 26.36 ± 0.01 A.

a, twice the distance between two hexagonal close packed planes, c', and the density with composition for the lanthanum-gadolinium system.

Microstructures of lanthanum-gadolinium and lanthanum-yttrium alloys

The microstructures of alloys in the vicinity of the δ phase were examined to check the results of X-ray diffraction and thermal analysis. Figure 11 is a photomicrograph of a 62.4 atomic percent yttrium alloy slow-cooled from the single phase β region to room temperature. Figure 12 and 13 show the two phase alloys, $\delta + \alpha$ Y and $\delta + \alpha$ La, containing 59.0 and 46.0 atomic percent yttrium respectively, cooled rapidly from the single phase β region. It should be noted that the photomicrograph has a ridge structure indicative of a low temperature solid transformation. Figures 14 and 15 show photomicrographs of the analogous 81.8 and 62.5 atomic percent gadolinium rapidly cooled from the single β phase. They show a microstructure similar to the microstructure of the analogous yttrium alloys. Figures 16, 17 and 18 are photomicrographs of single phase alloys containing 49.6, 74.5 and 84.0 atomic percent gadolinium. The results of the X-ray study are also substantiated by the microstructure of a 58.4 atomic percent gadolinium alloy shown in Figure 19. It has a ridged structure typical of an alloy which has undergone a low temperature solid transformation.

Figure 11. Photomicrograph of the 62.4 atomic percent yttrium alloy. 200 magnification

Figure 12. Photomicrograph of the 59.0 atomic percent yttrium alloy, δ + α Y. 200 magnification

Figure 13. Photomicrograph of the 46.0 atomic percent yttrium alloy, δ + α La. 200 magnification

Figure 14. Photomicrograph of the 81.8 atomic percent gadolinium alloy, δ + α Gd. 200 magnification

Figure 11.

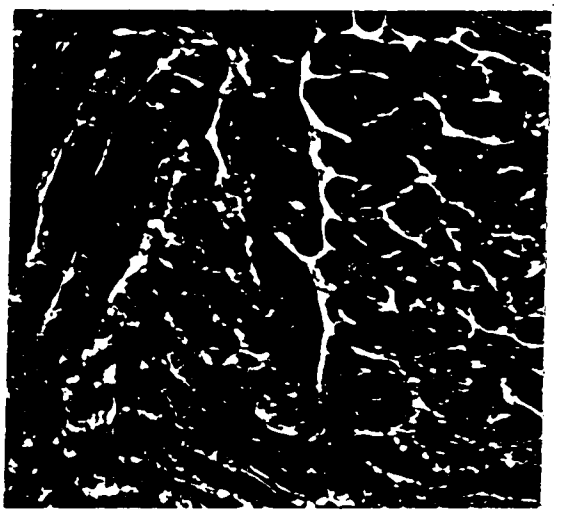

Figure 12.

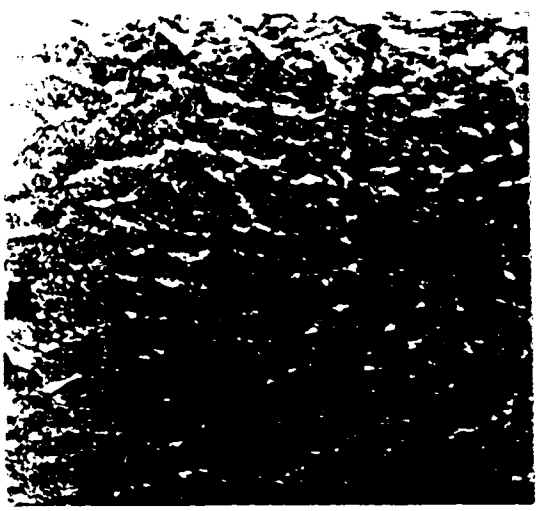

Figure 13.

Figure 14.

Figure 15. Photomicrograph of the 62.5 atomic percent gadolinium alloy, δ + α La. 200 magnification

Figure 16. Photomicrograph of the 49.6 atomic percent gadolinium alloy, α La. 200 magnification

Figure 17. Photomicrograph of the 74.5 atomic percent gadolinium alloy, δ. 200 magnification

Figure 18. Photomicrograph of the 84.0 atomic percent gadolinium alloy, α Gd. 200 magnification

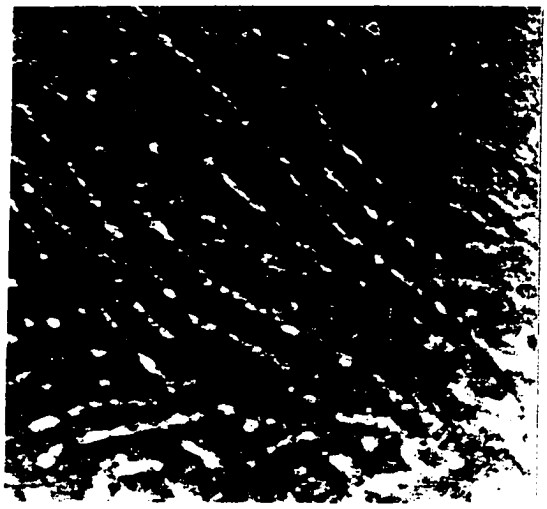

Figure 15.

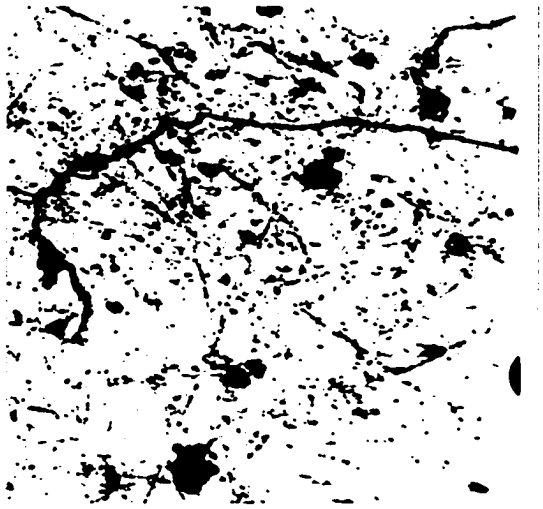

Figure 16.

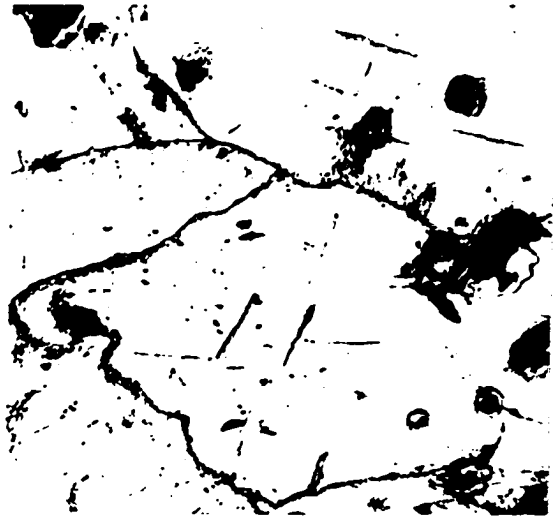

Figure 17.

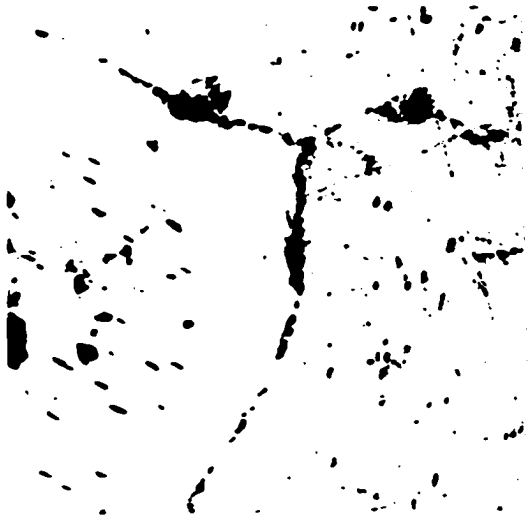

Figure 18.

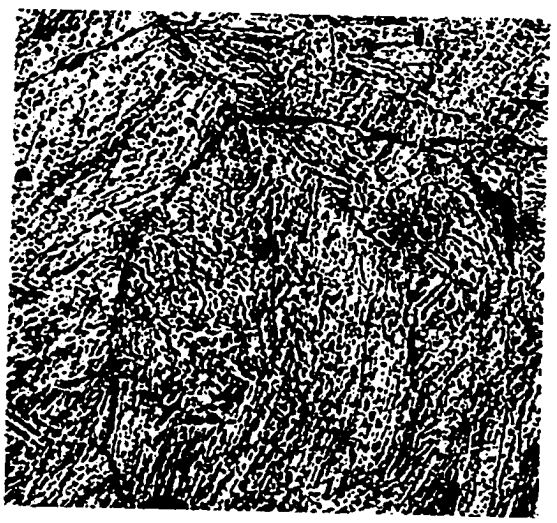

Figure 19. Photomicrograph of the 58.4 atomic percent gadolinium alloy, α La. 200 magnification

The Gadolinium-Yttrium System

The gadolinium-yttrium phase diagram consistent with the results of thermal analysis and the studies of the lanthanum-gadolinium and gadolinium-yttrium alloy systems is shown in Figure 20.

There is a region of β solid solubility above the $\alpha \rightarrow \beta$ transformations of gadolinium and yttrium. The alloys form a complete series of solid solutions below the β transformation. These results are exactly what one would predict from size and structure considerations and also from the study of the lanthanum-yttrium and lanthanum-gadolinium alloy systems. Figures 21, 22, 23 and 24 illustrate the variation in a, c, c/a and density versus composition determined from room temperature X-ray patterns of the alloys.

The thermal analysis results were extremely reproducible and the X-ray patterns were the best obtained from the three systems, lanthanum-gadolinium, lanthanum-yttrium and gadolinium-yttrium.

The δ Phase in Other Binary Intra-Rare Earth Alloys

Several alloys were made and their structure determined to check the possibility of other stacking arrangements than the δ occuring in the transition from one stacking arrangement to another. The cerium-yttrium alloy system was first

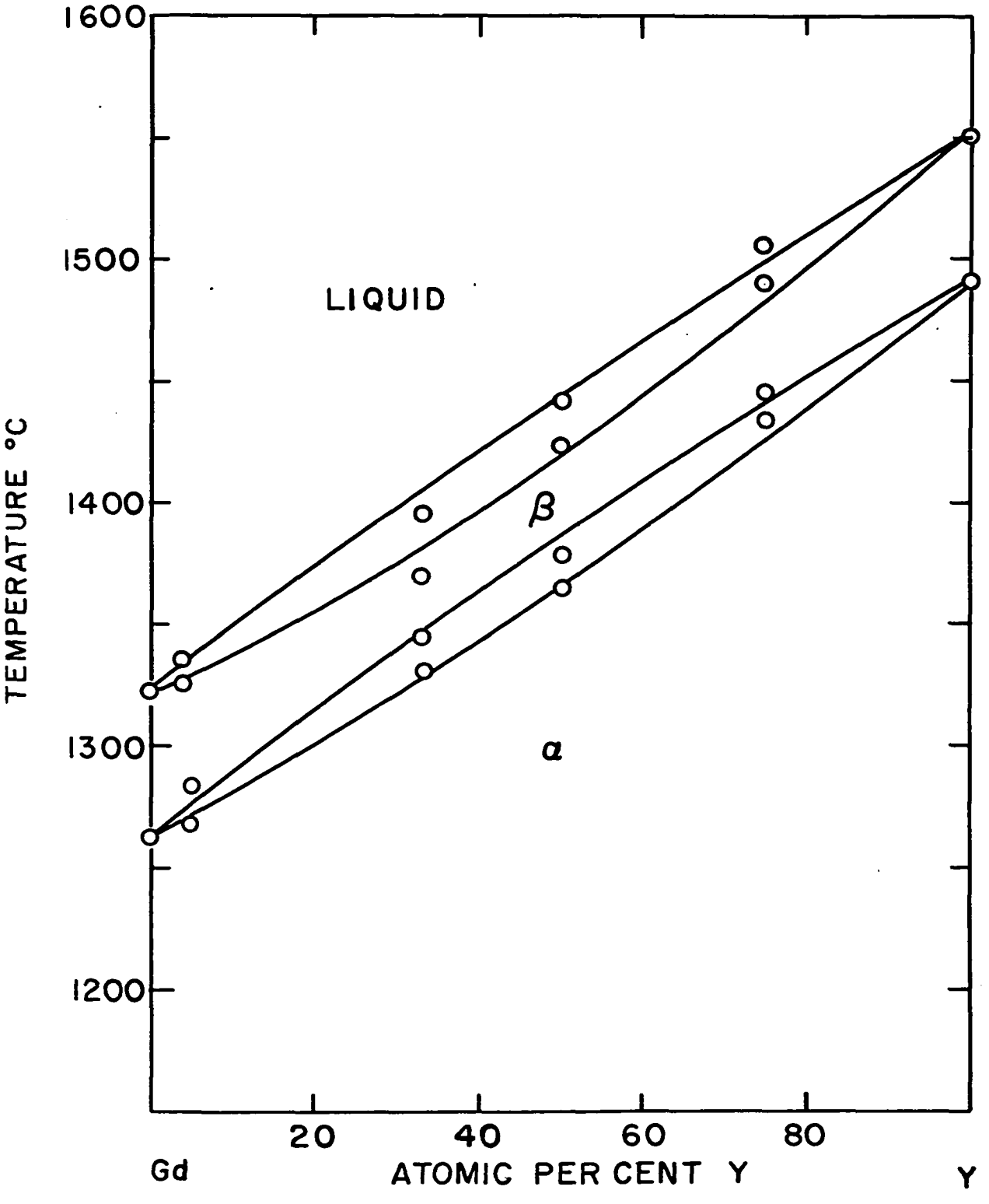

Figure 20. Phase diagram of the Gd-Y system

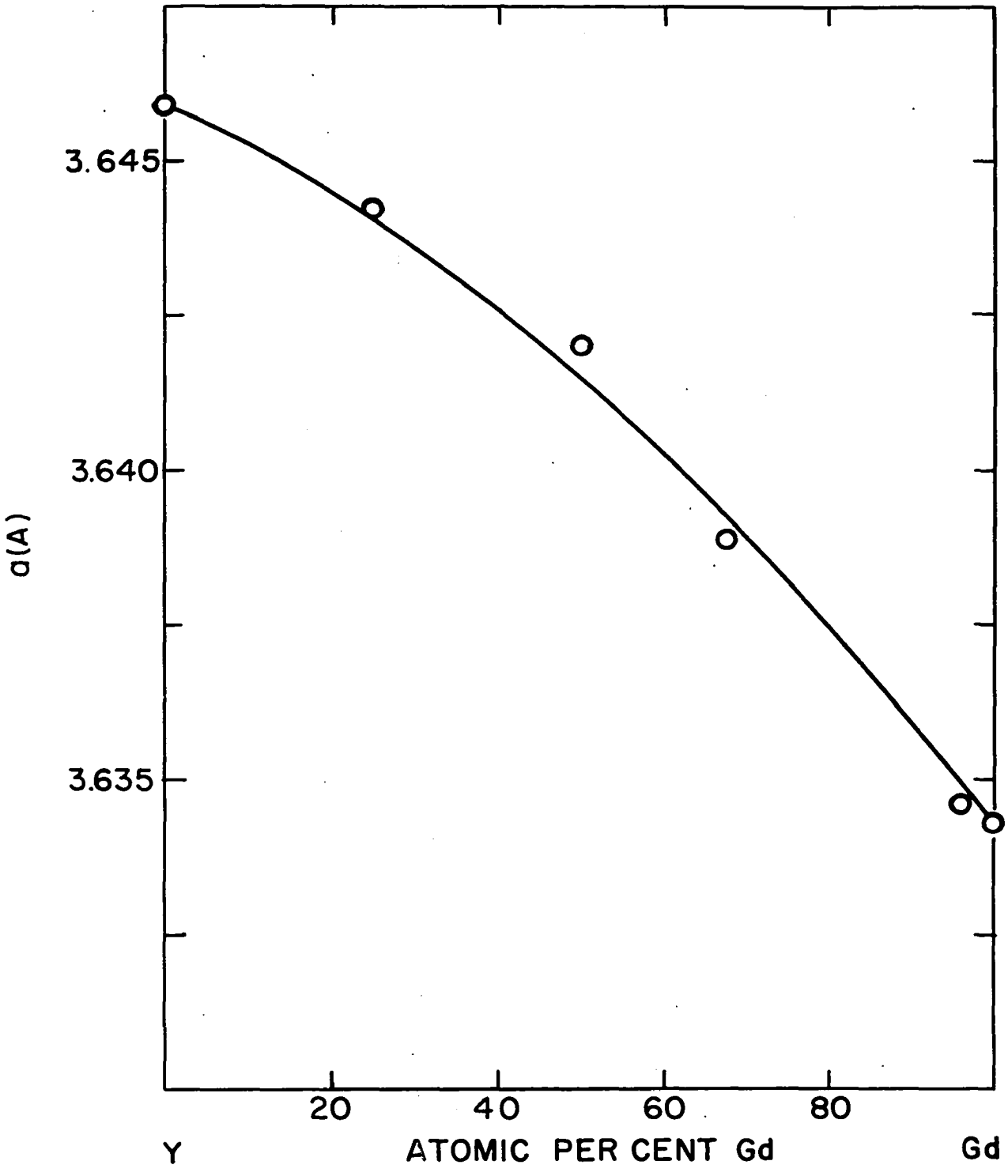

Figure 21. a vs. composition of the Gd-Y system

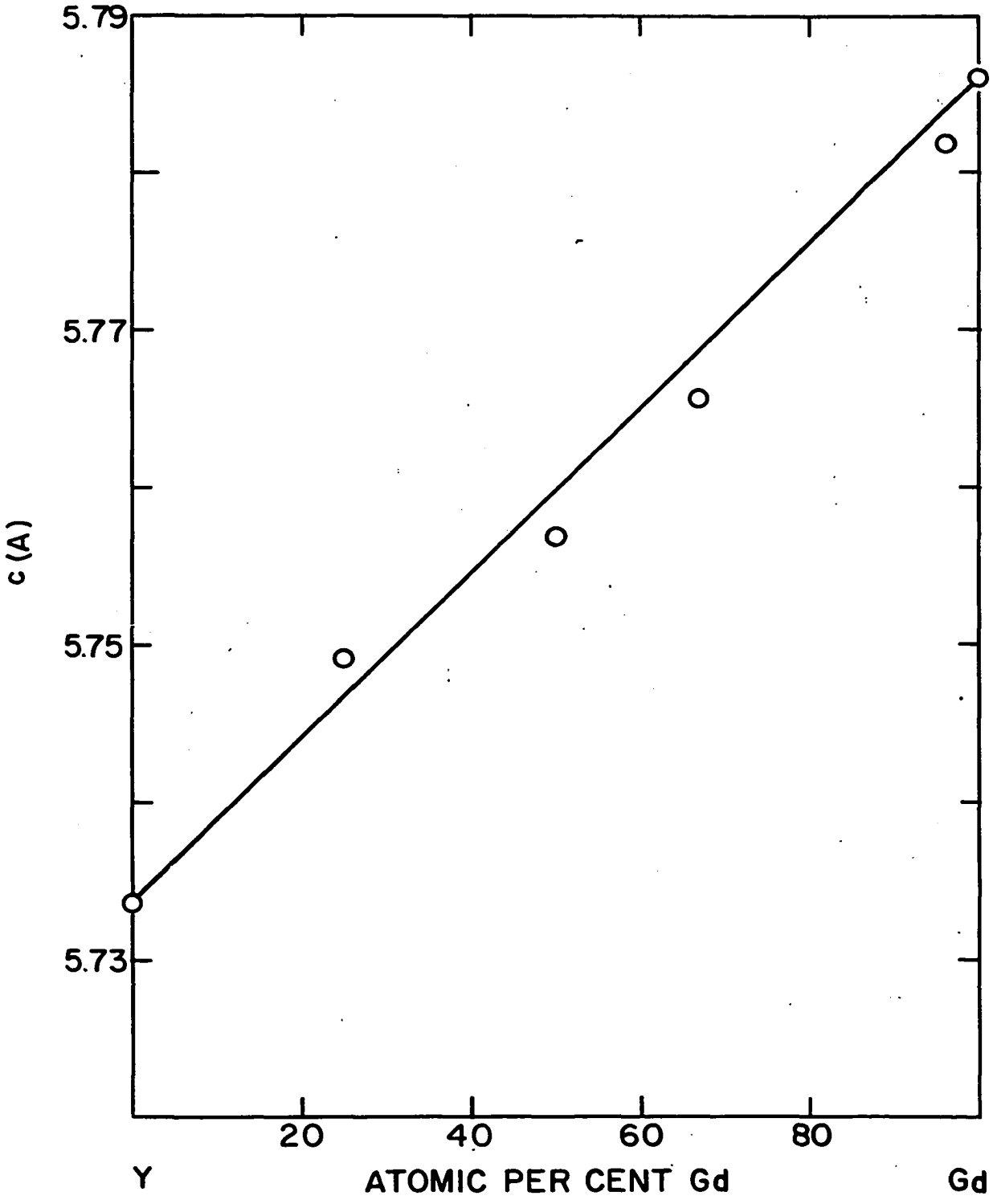

Figure 22. c vs. composition of the Gd-Y system

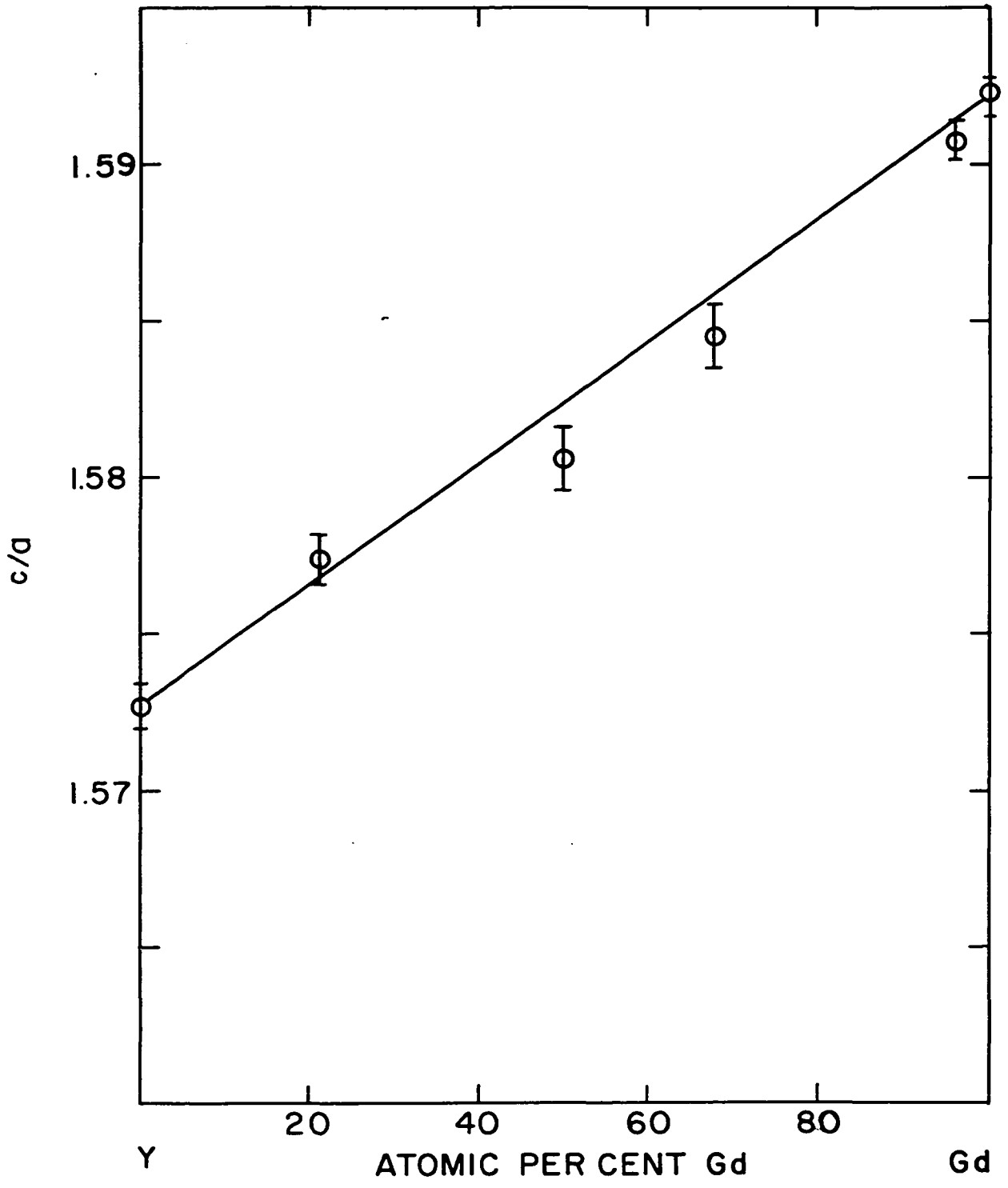

Figure 23. c/a vs. composition of the Gd-Y system

Figure 24. Density vs. composition of the Gd-Y syste

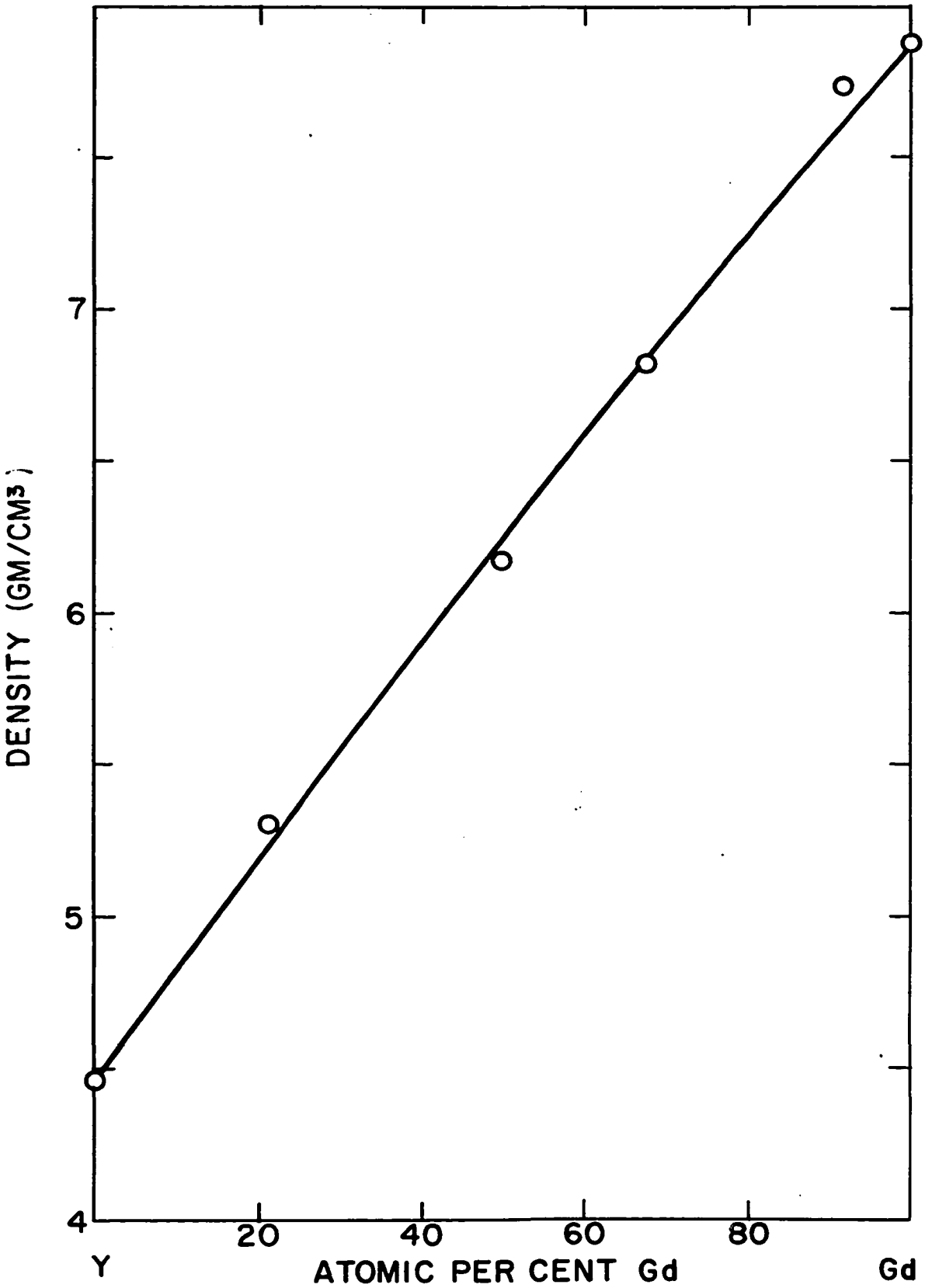
DENSITY (GM/CM³)
7
6
5
4
20
40
60
80
Y
ATOMIC PER CENT Gd
Gd

studied since the possibility existed that the samarium structure was formed in alloys only when a change in structure from the ABAC to ABAB stacking arrangement of the constituent metals was present. A 55.5 atomic percent yttrium-44.5 atomic percent cerium alloy was prepared by the method described earlier and a powder pattern of a sample prepared by the same method used for the systems already described was obtained. The alloy was indexed as a δ phase alloy with the lattice constants a = 3.653 $\pm$ 0.007 A and c = 26.55 $\pm$ 0.02 A. The results of this indexing are shown in Table 11. Alloys of praseodymium and neodymium with yttrium were also prepared to check the possibility of the formation of different stacking arrangements. The δ phase was found in the alloys studied, 49.7 atomic percent praseodymium-50.3 atomic percent yttrium and 53.0 atomic percent neodymium-47.0 atomic percent yttrium. The results of the indexing are shown in Tables 12 and 13.

As a result of vapor pressure studies of thulium-neodymium alloys, Barton (1957) inferred that a two phase α Tm + α Nd region was present in the system. He indexed a powder pattern of a 37 atomic percent thulium alloy as a mixture of these two phases. However, there were several lines which could not be indexed on this basis. Since the sample was prepared by filing the alloy in the air, he attributed these lines to an impurity phase. Since it appeared that a δ phase might be formed in this system and this might explain the extra lines found by Barton, his film was re-checked. The

Table 11. X-ray diffraction data of 55.5 atomic percent yttrium alloy

Int.	hkl	$\sin^2\theta$ observed	$\sin^2\theta$ [a] calculated	$\Delta\sin^2\theta$ observed-calculated
s	00,9	0.0696	0.0682	0.0013
vvw	10,4	0.0741	0.0729	0.0012
vvw	10,5	0.0809	0.0805	0.0004
vvw	10,10	0.1433	0.1437	-0.0003
vvw	10,11	0.1613	0.1614	-0.0001
w	11,0	0.1783	0.1783	0.0000
vw	10,13	0.2032	0.2019	0.0013
vw	10,14	0.2254	0.2246	0.0008
m	11,9	0.2474	0.2466	0.0008
vvw	20,5	0.2572	0.2588	-0.0015
w	10,16	0.2773	0.2752	0.0021
vvw	21,4	0.4316	0.4295	0.0020
vw	11,18	0.4515	0.4514	0.0000
vvw	21,14	0.5828	0.5813	0.0015
vvw	30,9	0.6043	0.6032	0.0010
vvw	22,9	0.7820	0.7815	0.0004
vvw	20,26	0.8050	0.8066	-0.0016

[a]Calculated using lattice constants, a = 3.658 ± 0.007 A and c = 26.55 ± 0.02 A.

pattern was indexed as a mixture of the δ phase and the α Nd structure. The results of this indexing are shown in Table 14.

Table 12. X-ray diffraction data of 50.3 atomic percent yttrium alloy

Int.	hkl	$\sin^2\theta$ observed	$\sin^2\theta$ calculated[a]	$\Delta \sin^2\theta$ observed-calculated
s	00,9	.0705	.0690	.0015
vvw	10,4	.0753	.0731	.0021
vw	10,5	.0811	.0808	.0002
vvw	10,10	.1443	.1447	-.0003
vw	110	.1796	.1786	.0010
w	10,13	.2047	.2035	.0016
vvw	10,14	.2266	.2265	.0001
w	119	.2497	.2476	.0020
w	10,16	.2789	.2776	.0013
vvw	21,4	.4321	.4304	.0016
m	21,5	.4382	.4381	.0000
vvw	10,23	.5113	.5101	.0011
vvw	00,27	.6209	.6209	.0000
vvw	21,22	.8280	.8277	.0002

[a]Calculated using lattice constants, a = 3.648 $\pm$ 0.007 A and c = 26.41 $\pm$ 0.04 A.

Table 13. X-ray diffraction data of 47.0 atomic percent yttrium alloy

Int.	hkl	$\sin^2\theta$ observed	$\sin^2\theta$ calculated[a]	$\Delta \sin^2\theta$ observed-calculated
s	00,9	0.0687	0.0688	-0.0000
s-	10,4	0.0732	0.0725	0.0006
s	10,5	0.0801	0.0802	-0.0000
vvw	10,8	0.1130	0.1133	-0.0002
vvw	10,10	0.1433	0.1439	-0.0005
m	10,13	0.2025	0.2025	0.0000
w	10,14	0.2254	0.2254	0.0000
m-	11,9	0.2459	0.2457	0.0001
vvw	20,5	0.2580	0.2571	0.0009
w-	00,18	0.2750	0.2752	-0.0002
w-	10,16	0.2750	0.2764	-0.0014
vvw	10,17	0.3046	0.3044	0.0001
vvw	20,10	0.3191	0.3208	0.0016
vw	20,16	0.4520	0.4533	-0.0013
vvw	21,8	0.4677	0.4672	0.0004
vw	10,23	0.5061	0.5083	-0.0022
vw	00,27	0.6209	0.6192	0.0016
vw	11,27	0.7981	0.7962	0.0018

[a]Calculated using lattice constants, a = 3.665 $\pm$ 0.007 A and c = 26.45 $\pm$ 0.02 A.

Table 14. X-ray diffraction data for 37 atomic percent thulium-63 atomic percent neodymium alloy

hkl Nd st.	hkl Sm st.	$\sin^2\theta$ observed	$\sin^2\theta$ [a] calculated Nd	$\sin^2\theta$ [b] calculated Sm
10,1	10,0	0.0600	0.0598	0.0592
00,4	10,2	0.0628	0.0627	0.0627
--	00,9	0.0693	--	0.0692
10,2	10,4	0.0729	0.0716	0.0729
--	10,5	0.0806	--	0.0806
10,3	--	0.0984	0.0912	--
00,5	10,7	0.1016	0.0979	0.1011
--	10,8	0.1139	--	0.1140
00,6	10,10	0.1448	0.1410	0.1448
10,5	--	0.1544	0.1539	--
--	11,0	0.1782	--	0.1778
--	10,13	0.2047	--	0.2038
20,1	10,14	0.2273	0.2277	0.2269
10,7	11,9	0.2480	0.2479	0.2471
00,8	20,4	0.2515	0.2508	0.2508
20,3	20,5	0.2589	0.2591	0.2585
--	10,16	0.2781	--	0.2782
--	00,18	0.2781	--	0.2771
20,5	20,10	0.3249	0.3218	0.3226
10,9	20,13	0.3826	0.3734	0.3816
21,2	20,14	0.4061	0.4074	0.4047
21,3	21,4	0.4300	0.4269	0.4286
10,10	--	0.4418	0.4478	--
--	21,5	0.4418	--	0.4363
21,4	11,18	0.4560	0.4544	0.4549
20,8	10,22	0.4748	0.4746	0.4732
--	10,23	0.5146	--	0.5117

[a]Calculated using lattice constants, a = 3.76 ± 0.007 A and c = 12.325 ± 0.01 A.

[b]Calculated using lattice constants, a = 3.656 ± 0.003 A and c = 26.36 ± 0.02 A.

Table 14. (Continued)

hkl Nd st.	hkl Sm st.	$\sin^2\theta$ observed	$\sin^2\theta$ [a] calculated Nd	$\sin^2\theta$ [b] calculated Sm
21,6	30,0	0.5359	0.5328	0.5335
10,11	--	0.5359	0.5301	--
00,12	21,13	0.5614	0.5643	0.5595
11,10	--	0.5614	0.5597	--
00,13	20,22	0.6526	0.6623	0.6510
00,14	20,25	0.7718	0.7681	0.7716
10,14	31,8	0.8235	0.8226	--

DISCUSSION

The phase diagrams proposed here for the three systems studied fit the empirical rules proposed by Hume-Rothery (1936) and others for predicting alloying behavior. Since the rare-earth metals and yttrium are similar in most of their properties, such as metallic radii, heats of fusion, number of valence electrons and structures, it would be predicted that: (1) there would be extensive solid solubility in the lanthanum-yttrium and lanthanum-gadolinium systems but not complete solid solubility at room temperature since the room temperature structures of the component metals is different, (2) there would be complete solid solubility in the gadolinium-yttrium system, (3) all the systems would show complete liquid miscibility, (4) addition of gadolinium or yttrium should increase the α - α' transformation temperature of lanthanum, (5) a region of complete solid solubility would exist below the liquid region of all three systems, if the elements have the same high temperature structure. However, it is not possible to predict the formation of a phase with an intermediate stacking arrangement of the type found here by any of the above empirically observed rules.

The transition of yttrium to a body centered cubic structure at high temperatures indicated by the study of the lanthanum-yttrium and gadolinium-yttrium systems has also been noted in the studies of Eash (1959) and Gibson (1959). The

extrapolation of the thermal data obtained for these two systems indicates a transformation temperature of 1490 $\pm$ 20° C which agrees very well with the studies of Eash. The study of the lanthanum-gadolinium system indicates that the high temperature structure of gadolinium is also body centered cubic.

High temperature transitions have been found by Hanak (1959) in all the rare-earth metals except europium, erbium and thulium. He has shown that lanthanum, cerium, praseodymium, neodymium and ytterbium have a body centered cubic structure below their melting point. Since this study has shown that yttrium and gadolinium have high temperature body centered cubic structures, it is reasonable to expect that all the rare-earth metals exhibiting a high temperature transformation transform to body centered cubic. The body centered transformation appears to be an accomodation of the lattice to the increased thermal vibrations of the atoms. If we assume that nearest neighbor interactions are not greatly dependent on structure, the change from 12 coordination in the close packed structures to 8 in the body centered cubic structure would allow larger thermal vibrations.

It is interesting that the change in stacking of a binary rare earth alloy system composed of a light rare earth and a heavy rare earth or yttrium should show an intermediate stacking or transition stacking similar to the samarium structure. This behavior is similar to the stacking change encountered

with increasing atomic number in the pure tri-valent rare-earth metals. This indicates that the samarium stacking arrangement is a transition between that of the light and heavy rare-earth metals.

This analogy between the pure metals and the alloys also is evident in another structural property, the c/a ratio. Figure 25 illustrates the variation in the c/a ratio versus composition for the lanthanum-yttrium and lanthanum-gadolinium systems. Comparison with the c/a ratio of the pure metals shown in Figure 26 shows this similarity. The values for the pure metals are taken from the structure study of Spedding et. al. (1956) except for samarium which was calculated from the lattice constants determined by Ellinger and Zacharaisen (1953). Daane et. al. (1954) report a c/a of 1.611 for samarium. It will be noted that the ABAC...hexagonal close packed structure is found with a c/a ratio of 1.612 or greater. The samarium structure is stable with a c/a ratio varying from 1.602 to 1.609, while the ABAB...hexagonal structure is found only when the c/a is below 1.594. The c/a ratio of Ce, Eu, and Yb are not shown in Figure 26 since they are not hexagonal at room temperature. However, McHargue et. al (1957) have observed a transformation in Ce to an ABAC hexagonal structure just below the ice point. They report values of a = 3.68 A, c = 11.92 A, and c'/a = 1.620 (c' = $\frac{1}{3}$c), which again agrees with the empirically observed rule that c/a must be greater than 1.612 for the ABAC...hexagonal structure.

Figure 25. c/a vs. composition of the La-Y and La-Gd systems

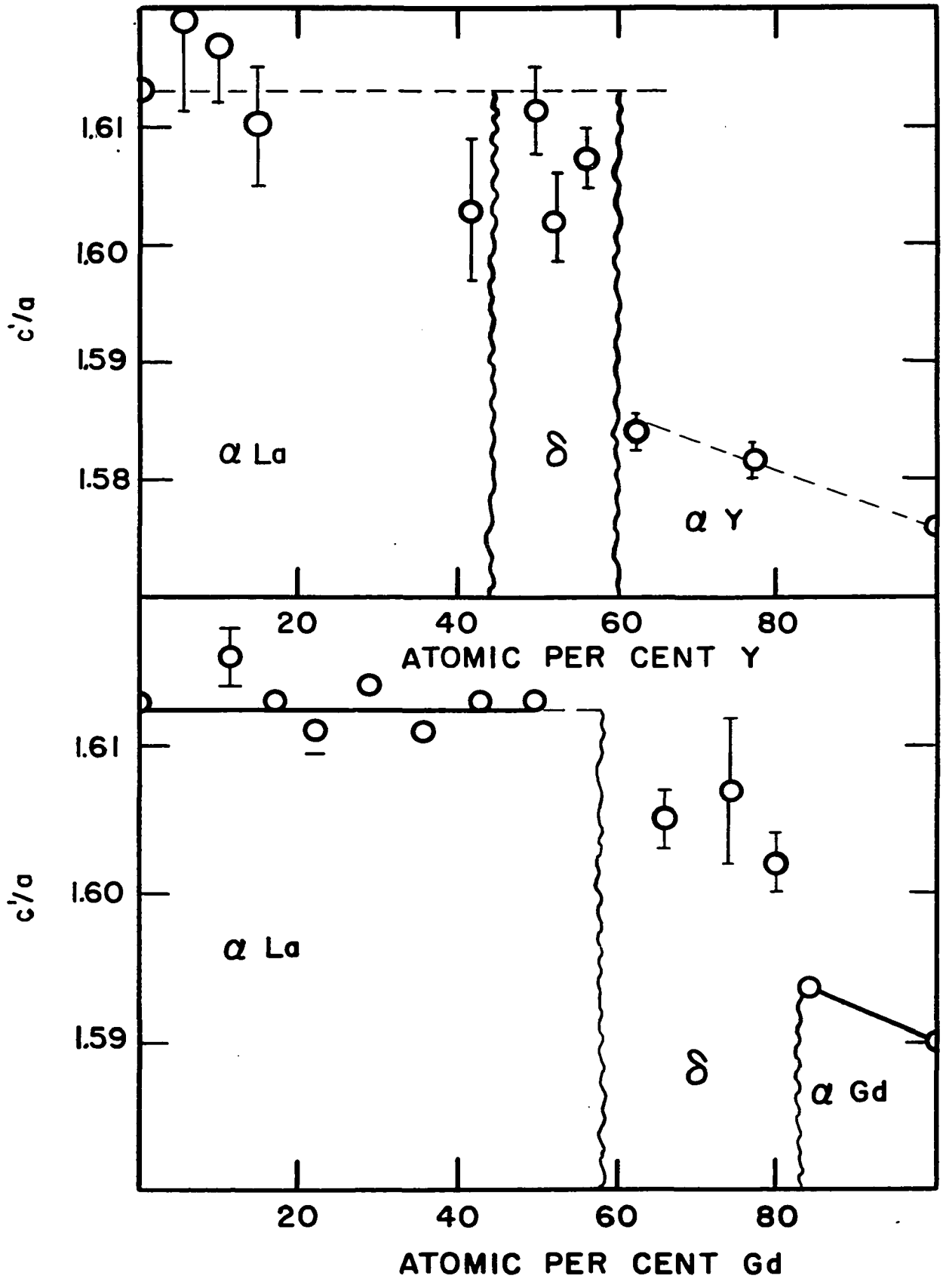
c'/a
1.61
1.60
1.59
1.58
α La
δ
α Y
20
40
60
80
ATOMIC PER CENT Y
c'/a
1.61
1.60
1.59
α La
δ
α Gd
20
40
60
80
ATOMIC PER CENT Gd

Figure 26. c/a of the pure rare-earth metals

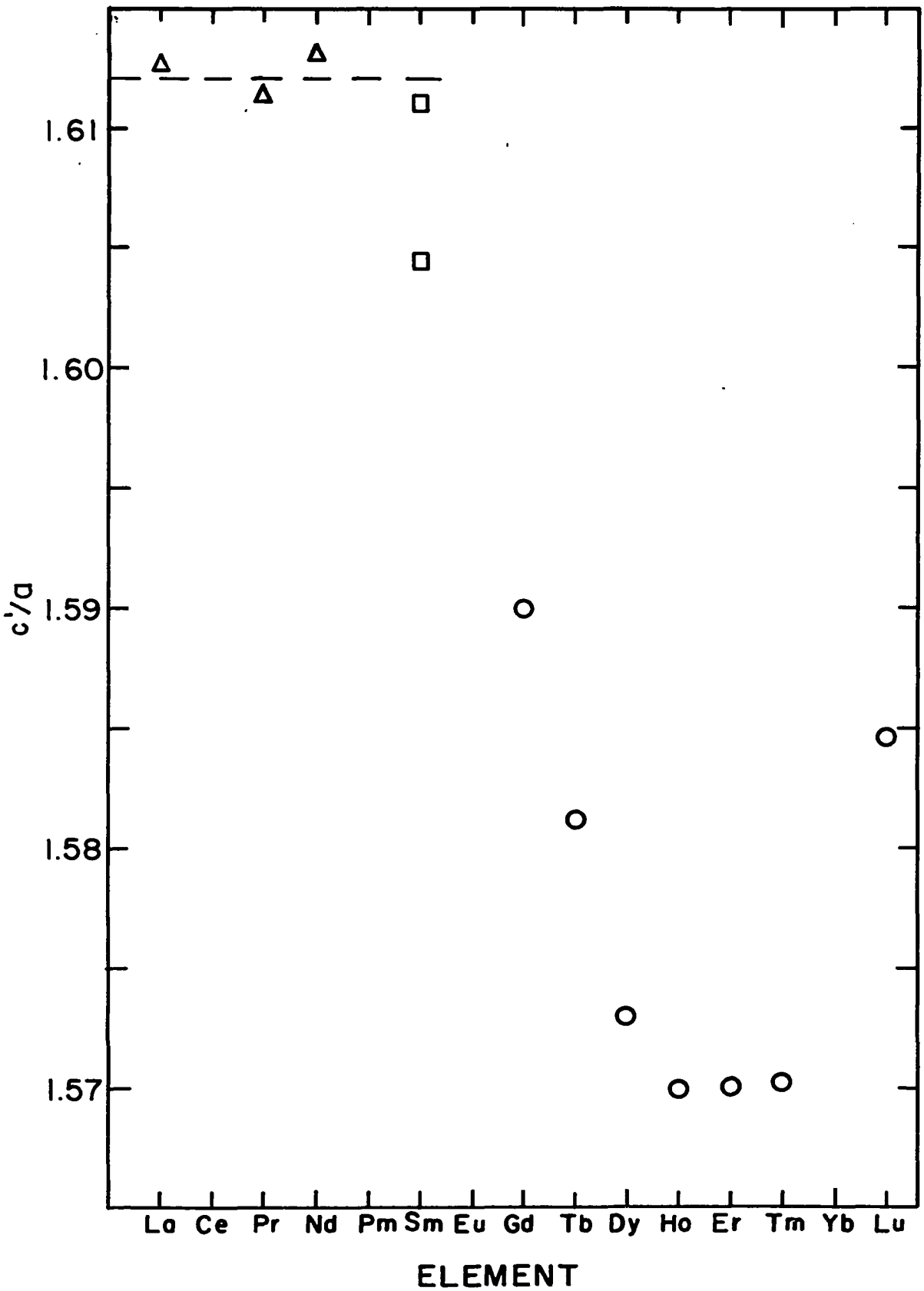
1.61
1.60
1.59
1.58
1.57
c'/a
La Ce Pr Nd Pm Sm Eu Gd Tb Dy Ho Er Tm Yb Lu
ELEMENT

This correlation of c/a ratio and structure suggests that the explanation might possibly be related to the Brillouin zone structure structure of the metals and alloys. Jones and Wills (1934) have shown that the number of electrons required to fill the Fermi sphere inscribed in the first Brillouin zone of an ABAB...hexagonal close packed metal is given by the following relation:

$$n = 2\text{-}3/4\ (a/c)^2 \left[(1-\tfrac{1}{4}(a/c)^2)\right] \qquad (1)$$

Thus, it can be seen that the ideal c/a ratio of 1.633 gives a value of 1.747 for n. However, most of the elements of the periodic table with the hexagonal close packed structure have 2 or more valence electrons, indicating that the electrons overlap the first and second Brillouin zone. Jones and Wills (1934) also have shown that the direction of overlap is determined by whether c/a is larger or smaller than the ideal value of the c/a ratio. Since most of the rare earth metals have a valence of 3, the physical picture is not clear, but it does indicate a relationship between the c/a ratio and the directional properties of the electron energy and distribution. Although the above discussion is only valid for ABAB hexagonal close packed structures, the similarity between all the close packed structures suggests this treatment should be valid in these structures also.

The results of this study indicate very clearly that the 4f electrons do not have a direct effect on the stacking

arrangements found in the pure metals and alloys, since yttrium does not have 4f electrons and the 4f orbitals of yttrium are so high in energy, they should not hybridize to give any directional bonding of the Pauling type. The stacking arrangements are not directly determined by the average atomic volume of the metal or alloy. Although the δ phase is stable at different compositions in the lanthanum-gadolinium and lanthanum-yttrium systems, the atomic volumes of yttrium and gadolinium are almost identical. Thus, yttrium in its effect on the structure of the alloys of the lanthanum-yttrium system seems to parallel the effect expected for holmium and dysprosium. This similarity is also found in the ionic radius of these elements. According to Goldschmidt (1927), the ionic radius of yttrium is intermediate to that of dysprosium and holmium. A more important factor is the c/a ratios of the three elements are almost the same. This suggests that the charge density on the surface of the ion might have some effect in determining the structure assumed by the metal or alloy. Since the c/a ratio changes with structure, the structure variations might result from a change in the number of electrons in the second Brillouin zone. Thus, it appears that a size factor effect is present in these alloys but the exact behavior is too complex to be determined from the results of this study. Further studies of the alloy systems should help elucidate the size factor effect.

LITERATURE CITED

Anderson, G. S., S. Legvold and F. H. Spedding, (1958). Phys. Rev. 109, 243.

Banister, J. R., S. Legvold and F. H. Spedding, (1954). Phys. Rev. 94, 1140.

Barton, R. J., (1957). Vapor pressure of thulium metal and some of its alloys. Unpublished Ph. D. Thesis. Ames, Iowa, Library, Iowa State University of Science and Technology.

Bommer, H., (1939). Z. Elektrochem. 45, 357.

Born, H., (1958). Thermal expansion of La-Y alloys. Unpublished M. S. Thesis. Ames, Iowa, Library, Iowa State University of Science and Technology.

Buerger, M. J., N. W. Buerger and F. G. Chesley, (1943). Am. Mineralogist 28, 285.

Cohen, M. U., (1935). Rev. Sci. Instr. 6, 68.

Cohen, M. U., (1936). Rev. Sci. Instr. 7, 155.

Daane, A. H., R. E. Rundle, H. G. Smith and F. H. Spedding, (1954). Acta Cryst. 7, 532.

Dash, D. T. (1959). Thorium-yttrium alloy system. Unpublished Ph. D. Thesis. Ames, Iowa, Library, Iowa State University of Science and Technology.

Ellinger, F. H. and W. H. Zacharaisen, (1953). J. Am. Chem. Soc. 75, 5650.

Farr, J. D., A. L. Giorgi and M. G. Bowman, (1953). The crystal structure of actinium and actinium hydride. U. S. Atomic Energy Commission Report LA-1545 [Los Alamos Scientific Laboratory].

Foex, M., (1944). Compt. rend. 219, 117.

Gibson, E. D., (1959). The yttrium-magnesium alloy system. To be published in Trans. Am. Soc. Metals [ca. 1959].

Goldschmidt, V. M., (1927). Ber. 60, 1263.

Habermann, C. E., A. H. Daane and F. H. Spedding, (1959). Melting point of yttrium. Research Notebook No. 4. (Manuscript) Ames, Iowa, Ames Laboratory of the U. S. Atomic Energy Commission, Iowa State University of Science and Technology.

Hanak, J. J., (1959). High temperature allotropy of the rare-earth elements. Unpublished Ph. D. Thesis. Ames, Iowa, Library, Iowa State University of Science and Technology.

Hume-Rothery, W., (1936). "The Structure of Metals and Alloys," London, Institute of Metals.

Jaeger, F., J. A. Bottema and E. Rosenbohm, (1938). Rec. Trav. Chim. Pays-Bas 57, 1137.

James, N. R., S. Legvold and F. H. Spedding, (1952). Phys. Rev. 88, 1092.

Klemm, W. and H. Bommer, (1937). Z. anorg. u. allgem. Chem. 231, 138.

Lock, J. M., (1957). Phil. Mag. 2, 726.

Massenhausen, W. v., (1952). Z. Metallkunde 43, 53.

McHargue, C. J., H. L. Yakel, Jr. and L. K. Jetter, (1957). Acta Cryst. 10, 832.

McLennan, J. C. and R. W. McKay, (1930). Trans. Roy. Soc. Can. Sect. 3, 24, 33.

Pirani, M. and H. Alterthum, (1923). Z. Elektrochem. 29, 5.

Quill, L. L., (1932a). Z. anorg. u. allgem. Chem. 208, 59.

Quill, L. L., (1932b). Z. anorg. u. allgem. Chem. 208, 273.

Roberts, L. M. and J. M. Lock, (1957). Phil. Mag. 2, 811.

Rossi, A., (1934). Nature (London) 133, 174.

Savitskii, E. M. and V. F. Terekhova, (1958). Zhurnal Neorganicheskai Khimii 3, 756.

Spedding, F. H. and A. H. Daane, (1954a). J. Metals 6, 504.

Spedding, F. H., and A. H. Daane, (1954b). Quarterly summary research report in metallurgy for January, February and March. U. S. Atomic Energy Commission Report I.S.C.-484 [Iowa State College].

Spedding, F. H. and A. H. Daane, (1956). In Finniston, H. M. and J. P. Howe, eds. "Progress in Nuclear Energy" Ser. 5, vol. 1, P. 413. London, England, Pergamon Press.

Spedding, F. H., A. H. Daane and K. W. Hermann, (1956). Acta Cryst. 9, 559.

Spedding, F. H., A. H. Daane and K. W. Hermann, (1957). J. Metals 9, 895.

Spedding, F. H., E. I. Fulmer, T. A. Butler and I. S. Jaffe, (1951). J. Am. Chem. Soc. 73, 4840.

Spedding, F. H., E. I. Fulmer, J. E. Powell and T. A. Butler, (1950). J. Am. Chem. Soc. 72, 2349.

Spedding, F. H. and J. E. Powell, (1954). J. Metals 6, 1131.

Thoburn, W. C., S. Legvold and F. H. Spedding, (1958). Phys. Rev. 110, 1298.

Trombe, F. and M. Foex, (1943). Compt. rend. 217, 501.

van Vleck, J. H., (1932). "Theory of Electric and Magnetic Susceptibilities". Oxford, England, Clarendon Press.

Vogel, R. and T. Heumann, (1947). Z. Metallkunde 38, 1.

Vogel, R. and H. Klose, (1954). Z. Metallkunde 45, 633.

Wakefield, G. F., (1957). The melting point of yttrium. Research Notebook No. 1, (Manuscript) Ames, Iowa, Ames Laboratory of the U. S. Atomic Energy Commission, Iowa State University of Science and Technology.

Young, R. A. and W. T. Ziegler, (1952). J. Am. Chem. Soc. 74, 5251.

Ziegler, W. T., (1949). Georgia Inst. Tech., State Eng. Exp. Station. Office of Naval Research Tech. Report. No. 1.

Ziegler, W. T., R. A. Young and A. L. Floyd, Jr., (1953). J. Am. Chem. Soc., 75, 1215.

Zintl, E. and S. Neumayr, (1933). Z. Elektrochem. 39, 84.

ACKNOWLEDGMENTS

The author would like to express his appreciation to Dr. A. H. Daane and Dr. F. H. Spedding for their guidance and interest during the course of this study. The author is also indebted to G. Wakefield and C. Habermann for the preparation of most of the pure metals and to J. Hanak for aid in the use of the I. B. M. 650 electronic computor.